Universiteit Utrecht

Bachelor Physics and Astronomy

Modeling of soot concentration in firn in the Greenland ice sheet

Bachelor Thesis

Arthur Polder

Supervisor:

Dr. Willem Jan van de Berg
Institute for Marine and Atmospheric research Utrecht

8 August 2020

Abstract

The albedo of the firn layer on the Greenland ice sheet (GrIS) is affected by the impurity soot concentration in firn. This thesis describes the evaluation of a stand-alone firn layer model with a dynamically modelled soot distribution. The model is evaluated for different locations on the GrIS. Analysis of model cross sections of the firn makes clear that it remains challenging to make cross sections which are in line with observational cross sections. Analyzing the mean surface soot concentration during the melt season shows that the effect of the dynamic soot distribution is almost independent of the initial soot concentration but dependent of the location for which the simulation is performed. Comparing model data with observational data makes clear that it is possible to reduce the model bias in the upward shortwave radiation and albedo by choosing the right values for the model parameters. This reduction is optimal for Automatic Weather Station (AWS) S9, but still suboptimal for AWS sites S6 and S10. The biases can be reduced using both a static and dynamic soot distribution. Overall, a static soot concentration between 0.000 and 0.002 ppb seems to give the best results. Analysis of the sensitivity of the model shows that the albedo is more sensitive to changing soot concentrations than to changing soot removal rates. The obtained optimal parameter values have a different SMB at S9, but the suboptimal parameter values for S6 and S10 give more similar effects for the separate locations. The SMB is more sensitive to changing soot concentrations compared to changing soot removal rates. Along the K-transect the order size of the SMB sensitivity is 0.5 m w.e.yr^{-1}.

Contents

1 Introduction

The majority of Greenland is covered by an ice sheet. The Greenland ice sheet (GrIS) is the second largest ice sheet in the world, with only the Antarctic ice sheet being larger. A complete melt of the GrIs will cause a mean sea level rise of 7.4 meters (Shepherd et al., 2020). Because melting ice contributes to sea level rise, it is relevant to understand ice dynamics and surface mass balance processes concerning the GrIS. The usage of a climate model is a useful way to get a better understanding of the GrIS. Regional climate models are used to simulate weather dynamics for a region in more detail. In this thesis the Regional Atmospheric Climate Model (RACMO2) is used.

Large parts of the GrIS are covered by a firn layer, which grows due to precipitation and shrinks due to runoff and sublimation during the year. To simulate the dynamics of the firn layer RACMO2 was coupled to a firn layer model by Ettema et al. (2009). Until now the soot concentration was assumed to be the same for all model layers of the firn layer model. Often a homogeneous soot concentration of 0.050 ppb was used for model evaluations of RACMO2. However, Doherty et al. (2010) showed that soot in firn is not homogeneously distributed. They also showed that the soot concentration is in fact far lower than 0.050 ppb.

The aim of this thesis is to evaluate a firn layer model which includes a dynamic description of the soot distribution. Initially the plan was to pay attention to the following research questions:

- How can the diffusion of impurities in snow be modelled the best?
- Can we estimate the current impact of impurities on snowmelt?
- For which climate conditions is the impact of impurities the largest on snow melt?

However, during the project the focus was on the first two questions. Therefore this thesis focuses on these two questions and the third questions is not taken into consideration.

Chapter 2 introduces a few physical concepts which are important in polar climate physics. This chapter discusses measurements of the soot concentration in the firn layer obtained by Doherty et al. (2010). More information about the (data from) Automatic Weather Stations (AWS) is also included in this chapter. Chapter 3 gives more information about RACMO2 and explains the stand-alone version of the firn layer model in more detail. Chapter 4 presents the results of the simulation and makes a comparison with observational data. Chapter 5 discusses the obtained results and gives suggestions for further research. In chapter 6 the final conclusion is drawn.

2 Theory

Two important concepts in polar climate physics are the surface energy balance (SEB) and the surface mass balance (SMB). The SEB considers the incoming and outgoing energy at the surface and is mathematically described by:

$$\begin{aligned} \mathrm{M} &= \mathrm{SW_d} - \mathrm{SW_u} + \mathrm{LW_d} - \mathrm{LW_u} + \mathrm{SHF} + \mathrm{LHF} + G_\mathrm{s}, \\ &= \mathrm{SW_n} + \mathrm{LW_n} + \mathrm{SHF} + \mathrm{LHF} + G_\mathrm{s}, \end{aligned} \tag{1}$$

where M is the SEB, $\mathrm{SW_d}$ and $\mathrm{SW_u}$ are the down- and upward shortwave radiation fluxes, $\mathrm{LW_d}$ and $\mathrm{LW_d}$ are the down- and upward longwave radiation fluxes, SHF and LHF are the sensible and latent heat fluxes and G_s is the subsurface heat flux. $\mathrm{SW_n}$ and $\mathrm{LW_n}$ are the net short- and longwave radiation fluxes. All fluxes are expressed in $\mathrm{W\,m^{-2}}$ and are defined positive (Noël et al., 2018).

The SMB considers the mass increase and decrease of the GrIS and is mathematically described by:

$$\mathrm{SMB} = \mathrm{SF} + \mathrm{RA} + \mathrm{SU} - \mathrm{RU}, \tag{2}$$

where SF is the snowfall, RA is the rain, SU is the sublimation and RU is the runoff. All quantities are defined positive, except for the sublimation. A positive sublimation means therefore deposition instead of sublimation. All SMB components are expressed in meter water equivalence per year ($\mathrm{m\,w.e.yr^{-1}}$).

The albedo (ALB) is the part of the downward shortwave radiation which is reflected by the surface. Mathematically this quantity is defined as:

$$\mathrm{ALB} = \mathrm{SW_u}/\mathrm{SW_d}, \tag{3}$$

where $\mathrm{SW_d}$ is the downward shortwave radiation flux and $\mathrm{SW_u}$ is the upward shortwave radiation flux. The albedo is dependent of the kind of surface. Snow has a high albedo, typically in the range of 0.70-0.90. Because the albedo of snow is generally spoken high, small amounts of light-absorbing impurities can dominate the absorption of solar radiation at visible wavelengths. This can reduce the albedo, causing an increase of the SEB, leading to an increasing amount of melt, which means a decreasing SMB (Doherty et al., 2010). Increased melt causes a decrease of the albedo, which causes an increase of the absorption of shortwave radiation again. This mechanism is called the melt-albedo feedback and is a positive feedback mechanism. This effect can be found at the southwestern ice sheet margin of the GrIS (Box et al., 2012). It is important to understand this mechanism, because the positive feedback mechanism amplifies ice melt.

Doherty et al. (2010) showed that the vertical distribution of snow impurities (soot) in the firn layer is not homogeneous. The result of their analysis of the vertical distribution of the soot concentration can be found in Figure 1. For almost all depths of the vertical sample the soot concentration is between 0.000 and 0.002 ppb (ng/g). However, the figure shows also an increase of soot concentration in the layer between 10 and 20 cm below the surface.

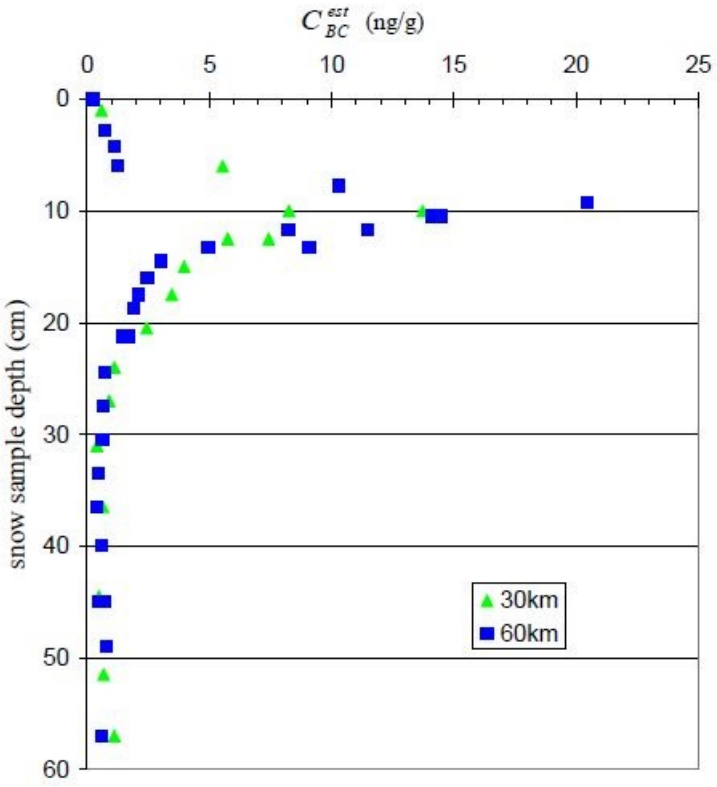

Figure 1: Vertical distribution of snow impurities in the firn layer 30 and 60 km below the Dye-2 station (Doherty et al., 2010).

Table 1: Latitude, longitude, height, distance from ice edge and period for which AWS data is available for locations used in this thesis to perform simulations (Noël et al., 2015; Kuipers Munneke et al., 2018).

AWS-location	latitude (°)	longitude (°)	Height (m a.s.l.)	Distance from ice edge (km)	AWS data period
S5	67.095	-50.009	490	6	-
S6	67.037	-49.456	1020	38	2003-2015
S9	67.032	-48.153	1520	88	2003-2015
S10	67.001	-47.103	1850	140	2009-2015
Summit	72.597	-38.670	-	-	-
Dye-2 60 km S	65.923	-44.709	-	-	-

Doherty et al. (2010) stated that small amounts of light-absorbing impurities can dominate the absorption of solar radiation. Therefore it is important to understand the distribution of soot in the firn layer. Until now the soot concentration was assumed (for more information about RACMO2 see chapter 3) to be the same for all levels of the firn layer in RACMO2. This thesis evaluates a firn layer model with a dynamic description of the soot concentration.

In this thesis simulations are only performed for a few locations and the model is not inte-

grated over the GrIS. The two samples discussed in Figure 1 were taken on locations 30 and 60 km south of AWS site Dye-2 on 25 July 2008 (Dohorty et al., 2010). Because most data points come from the sample taken 60 km south of Dye-2, simulations are performed for the gridbox (see chapter 3) where this location is situated. The other used gridboxes are the gridboxes where AWS sites S5, S6, S9, S10 and Summit are located. The stations S5, S6, S9 and S10 are located along the K-transect of western Greenland. The K-transact starts at the western edge of the GrIS, about 20 km east of Kangerlussuaq, and runs 140 km to the east (Kuipers Munneke et al., 2018). The locations of S5, S6, S9 and S10 are shown on the map in Figure 1.

AWS data is used from stations S6, S9 and S10. AWS data from stations S6 and S9 is available for the period 2003-2015 and from station S10 for the period 2009-2015. There are some data gaps in the AWS data, including an annual gap for the period around 21 December. The daily averages which are missing in the AWS data are also excluded from the model output to make a more reliable comparison between AWS and model data. Table 1 gives an overview of the stations used for model evaluations, including the coordinates of the locations. For S5, S6, S9 and S10 the height above the sea level and the distance from the ice edge are also included (Kuipers Munneke et al., 2018). For S6, S9 and S10 the period for which AWS data is available is also shown.

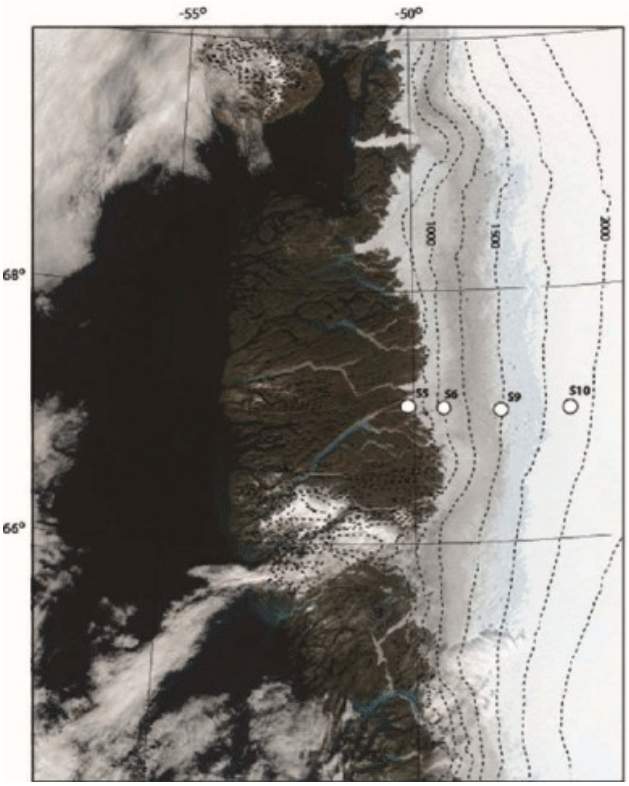

Figure 2: Locations of AWS stations S5, S6, S9 and S10 on the GrIS (Kuipers Munneke et al., 2018).

3 Model description and simulation set-up

3.1 RACMO2.3

In this thesis the Regional Atmospheric Climate Model version 2.3 (RACMO2) is used to make simulations of the GrIS. RACMO2 is developed at the Royal Netherlands Meterological Institute (KNMI) and is a combination of two weather models. The atmospheric dynamics come from the High Resolution Limited Area Model (HIRLAM), while the physical processes come from the European Centre for Medium-Range Weather Forecasts (ECMWF-IFS) (Noël et al., 2015).

Ettema et al. (2009) applied RACMO2 for the first time to the GrIS by using version 2.1 of RACMO. To apply RACMO2 to the GrIS a multilayer firn model was added to RACMO2, leading to a polar (p) version of RACMO2. Later the model was improved by the implementation of a validated albedo scheme (Kuipers Munneke et al., 2011). The replacement of RACMO2.1 by RACMO2.3 led to a new polar version of the model, RACMO2.3p1 (Noël et al., 2015). Further improvements resulted in version RACMO2.3p2 (Noël et al., 2018).

In this thesis data from an evalutation of RACMO2.3p1 is used (Noël et al., 2015), which is used to run the stand-alone version of the firn layer model of RACMO2.3p2.

The stand-alone version of the firn layer model is a multilayer snow model, simulating the processes in the firn layer on the GrIS. The model includes only a vertical distribution of soot, so it is a 1D model. Although the firn layer model includes no horizontal distribution, the model can be evaluated for different locations, using data of different gridboxes obtained by an evaluation of RACMO2.3p1 (Noël et al., 2015).

The simulated processes include mass accumulation due to snow and rain, percolation of meltwater from the surface into the firn, refreezing within the firn layer and runoff at the firn-ice interface. The albedo is calculated by using the albedo scheme described by Kuipers Munneke et al. (2011). The stand-alone firn layer model is a multilayer model. Each model layer has its own values for relevant quantities like water saturation, snow density and snow temperature.

One of the assumptions being made is that melt occurs only at the surface. Meltwater at the surface percolates into the firn and is retained by the firn until the maximum capillary water storage is reached. The maximum capillary water storage expresses how much liquid water the firn layer can contain. Each model layer has its own maximum capillary water storage due to the multiple layers of the model. When meltwater at the surface percolates into the firn layer, for each model layer is checked if the maximum capillary water storage is already reached. When the maximum capillary water storage is already reached, the meltwater goes down to the model layer below, until it reaches a model layer which is still unsaturated. When the meltwater reaches the firn-ice interface, the meltwater is assumed to runoff immediately. The meltwater refreezes at any subsurface layer with a temperature below the freezing point. The vertical displacement of water is assumed to take place in a single time step (Kuipers Munneke et al., 2014).

Replacing the statically modelled soot concentration by a dynamically modelled soot concentration means that the soot concentration is no longer the same for all model layers, but becomes a property of the model layer, like density and temperature.

The model has a few parameters to regulate the simulation of soot in the firn layer. The parameter RSOOT sets the initial soot concentration of the firn. This includes both the soot concentration of the firn layer at the beginning of the simulation period, as the soot concentration in fresh snow which falls down during the simulation period.

The parameter RS2W sets the soot removal rate. This parameter defines the fraction of the soot in the meltwater which percolates down with the meltwater into the firn. A RS2W-value of 0.00 means that no soot percolates into the firn with the meltwater, leading to a high soot concentration at the surface. A RS2W-value of 1.00 means that all soot percolates into the firn with the meltwater.

The firn layer model makes it also possible to simulate the penetration of downward shortwave radiation into the firn. However, radiation penetration is not taken into account in this thesis. All downward shortwave radiation is assumed to be absorbed or reflected at the surface.

Lastly, the firn layer makes it also possible to perform simulations with the original (static) soot distribution. This option is used to perform part of the simulations discussed in this thesis.

3.2 Initialization and set-up

As described above, data from an evaluation of RACMO2.3p1 (not RACMO2.3p2) was coupled to the stand-alone version of the firn layer model of RACMO2.3p2. RACMO2.3p1 was evaluated using a resolution of 11 km and 40 vertical layers. The integration domain included the GrIS, the Canadian Arctic Archipelago, Iceland and Svalbard. The output of this evaluation consisted of data of all evaluated gridboxes. More information about (an evaluation of) this model can be found in a paper by Noël et al. (2015). The simulation data used to perform the simulations discussed in this paper covers the period 1991-2015.

To evaluate the stand-alone firn layer model a gridbox has to be chosen for which the simulation is performed. The six gridboxes which are used to perform the simulations discussed in this thesis are described in more detail in chapter 2.

4 Results

4.1 Firn layer cross sections

Doherty et al. (2010) analyzed the vertical distribution of impurities by measuring the soot concentration in two firn columns. Their results were discussed in chapter 2 and shown in Figure 1. Because most data points in Figure 1 come from the sample taken 60 km south of Dye-2, simulations are performed for the gridbox where this location is situated.

Figure 3 shows six cross sections of the modelled firn layer of this gridbox, obtained by six simulations, using different RSOOT- and RS2W-values. All cross sections are based on model output belonging to 25 July 2008, because the snow sample was taken on this date. All cross sections show an increased soot concentration at the surface. The soot concentration increase at the surface is larger for higher initial soot concentrations and is lower for higher RS2W-values. This effect is not always visible, but becomes more clear if the initial soot concentration is higher and the change in RS2W-value is larger. This effect is illustrated by the difference between Figure 3e and 3f.

The most important difference between the observed and modelled cross sections is the place of the increased soot concentration in the firn layer. The cross section in Figure 1 shows an increased soot concentration in the layer between 10 and 20 cm below the surface, but all cross sections in Figure 3 show an increased soot concentration just below the surface.

An initial soot concentration of 0.001 ppb is generally in line with the soot concentration in Figure 1, except for the increased concentration in the layer between 10 and 20 cm below the surface. An initial soot concentration of 0.002 ppb gives a higher peak, but this peak is still too low. At other depths, the soot concentrations is a little too high compared to Figure 1. Simulations with an initial soot concentration of 0.005 ppb give high peak concentrations which are comparable with the peak concentration Figure 1 shows. However, for the other depths the concentration is far too high compared to Figure 1.

It is remarkable to see a soot concentration lower than the initial soot concentration just below the peak concentration in the modelled cross sections. This effect is very clear for the modelled cross sections with RSOOT = 0.005 ppb (Figure 3e and 3f). It seems, based on Figure 3, that this effect is stronger for low RS2W-values than for high RS2W-values. Although this effect was not investigated thoroughly, it is probably caused by the percolation of meltwater into the firn layer. For low RS2W-values clean meltwater percolates into the firn layer (the meltwater is clean because the soot stays at the surface) where it refreezes. Due to the refreezing of the meltwater the total mass of the layer increases. Beause the refrozen meltwater is clean, the total amount of soot does not increase. Therefore the soot concentration decreases.

Figure 4 shows cross sections of 1 April, 1 June, 1 August and 1 October 2008 for the same location. The model evaluations are performed with an initial soot concentration of 0.002 ppb and a RS2W-value of 0.20. On 1 April (Figure 4a) the cross section shows no increased soot concentration at the surface. Figure 4b shows the situation on 1 June, which is roughly the start of the melt season. On 1 June the soot concentration is higher in the upper 10 centimeter of the firn layer than in the rest of the firn. The cross section of 1 August (Figure 4c) shows even a higher concentration in the upper part of the firn layer. Figure 4d

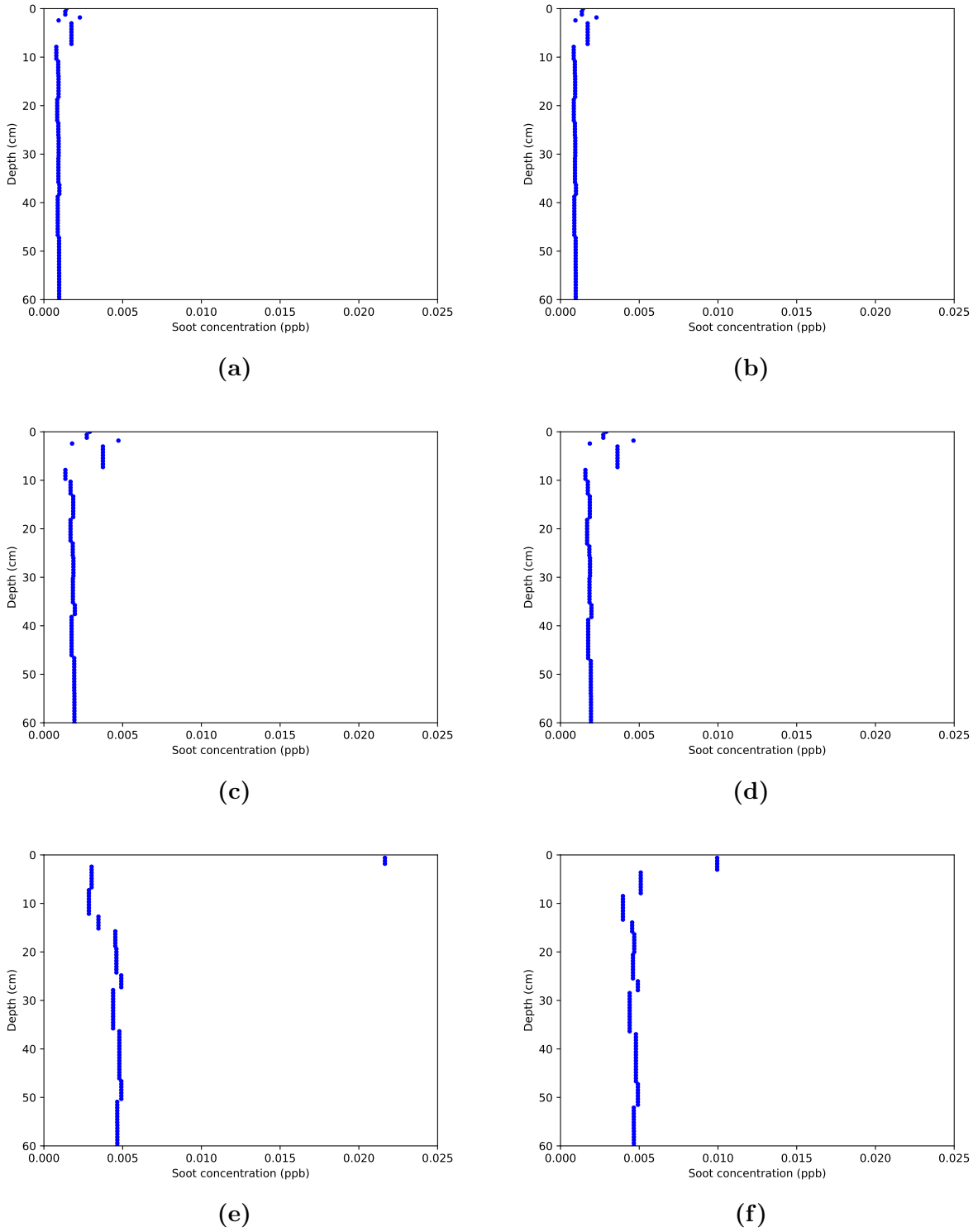

Figure 3: Modelled vertical soot distribution at a location 60 km south of Dye-2. All cross sections belong to 25 July 2008, but are based on simulations with different RSOOT- and RS2W-values: a) RSOOT = 0.001 ppb and RS2W = 0.30, b) RSOOT = 0.001 ppb and RS2W = 0.40, c) RSOOT = 0.002 ppb and RS2W = 0.10, d) RSOOT = 0.002 ppb and RS2W = 0.30, e) RSOOT = 0.005 ppb and RS2W = 0.20 and f) RSOOT = 0.005 ppb and RS2W = 0.70.

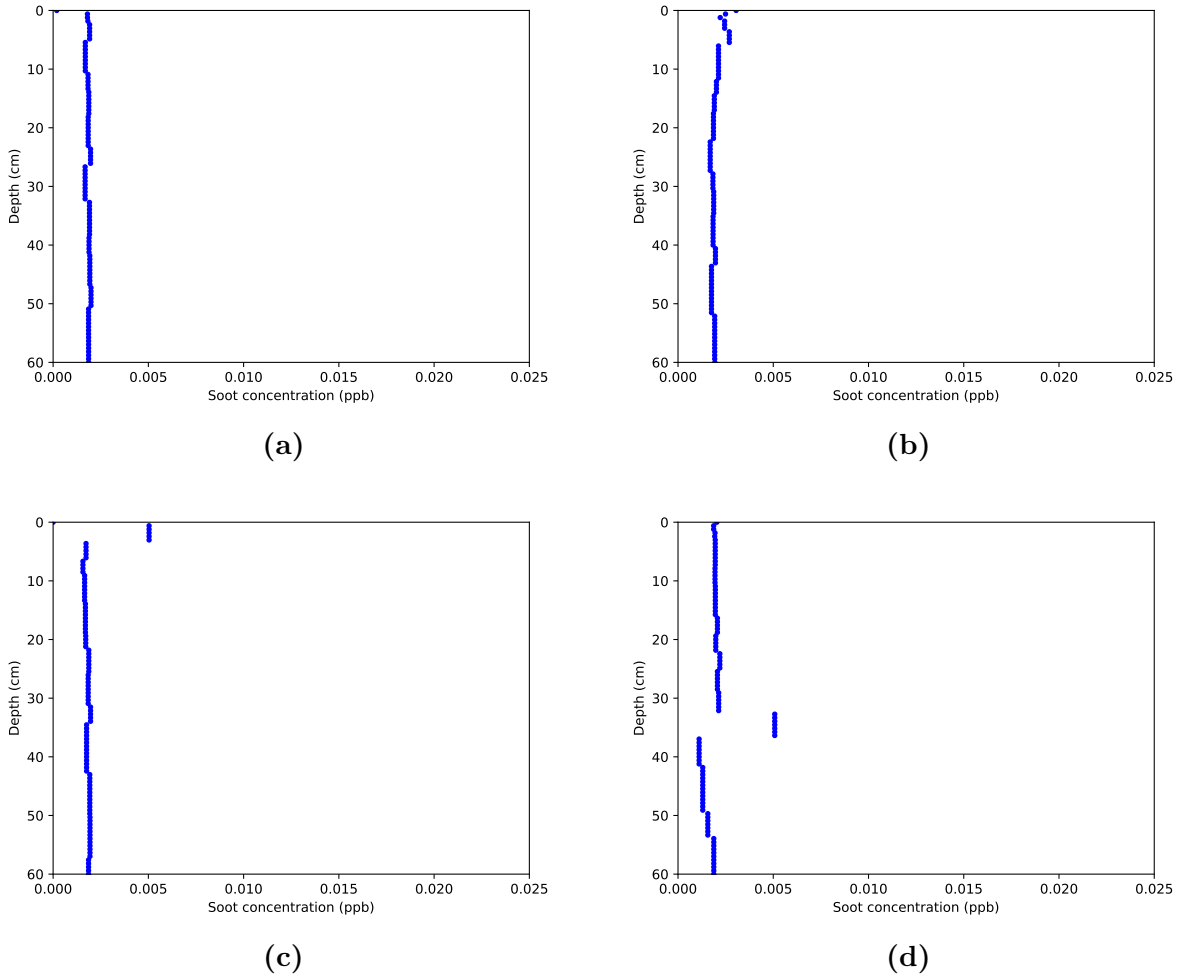

Figure 4: Modelled vertical soot distribution at a location 60 km south of Dye-2 for different moments in 2008. The simulations are performed with RSOOT = 0.002 ppb and RS2W = 0.20. The cross sections show the situation on a) 1 April, b) 1 June, c) 1 August and d) 1 October.

shows the situation on 1 October. Due to the precipitation of snow the soot concentration peak is located 30 cm lower in the firn layer. Figure 1 shows also a peak concentration which is not directly below the surface. However, this modelled cross section belongs to 1 October 2008 instead of 25 July 2008.

Figure 5 shows a cross section of a model evaluation for the gridbox where station S9 is located. This simulation is performed with an initial soot concentration of 0.001 ppb and a RS2W-value of 0.20. The cross section shows the situation on 10 September 1992. At S9 the melt is larger than 60 km south of Dye-2.

This cross section has a lot of similarities with the observational cross section in Figure 1. The cross section shows a soot concentration of 0.002 ppb below the peak. This concentration is a little too high but comparable with the soot concentration below the peak in Figure

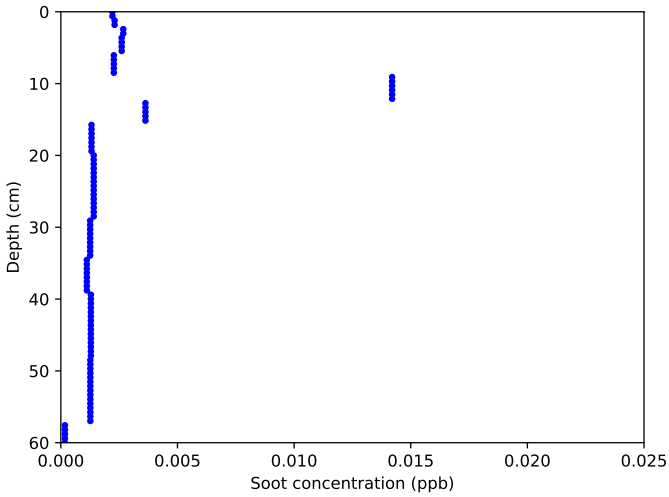

(a)

Figure 5: Modelled vertical soot distribution at S9 on 10 September 1992. The simulation is performed with RSOOT = 0.001 ppb and RS2W = 0.20.

1. The maximum peak concentration is roughly 0.014 ppb, which is lower than the peak concentration of roughly 0.020 ppb in Figure 1. Thirdly, the soot concentration is in both cross sections higher above the peak than below the peak.

Figure 5 makes clear that it is possible to make cross sections which are comparable with Figure 1 by using the dynamic soot concentration model. However, the problem is that Figure 5 is a cross section of a different location, and belongs to 10 September 1992 instead of 25 July 2008. So from this figure cannot be concluded that model cross sections are in line with the observational cross section on the same date and location for specific model parameters.

4.2 Soot concentration sensitivity

Comparing cross sections from model evaluations with the observational cross section remains challenging. Therefore it makes sense to use other methods to investigate the effect of the dynamic soot concentration. One of these methods is the analysis of the mean soot concentration at the surface during the melt season. This quantity is calculated by averaging the daily mean surface soot concentrations during the melt period. The daily mean surface soot concentration is one of the output quantities of the model. The melt season is in this thesis defined as the period from 1 June to 30 September.

To analyze the sensitivity of the mean surface soot concentration, the model is evaluated for different locations, using different initial soot concentrations and RS2W-values. The initial soot concentrations are 0.001, 0.002 and 0.005 ppb and the RS2W-values vary from 0.05 to 1.00, with steps of 0.05. The model is evaluated for the gridboxes where the stations S5, S6, S9, S10 and Summit are located.

Figure 6 shows the results of these simulations. All subfigures make clear that an initial

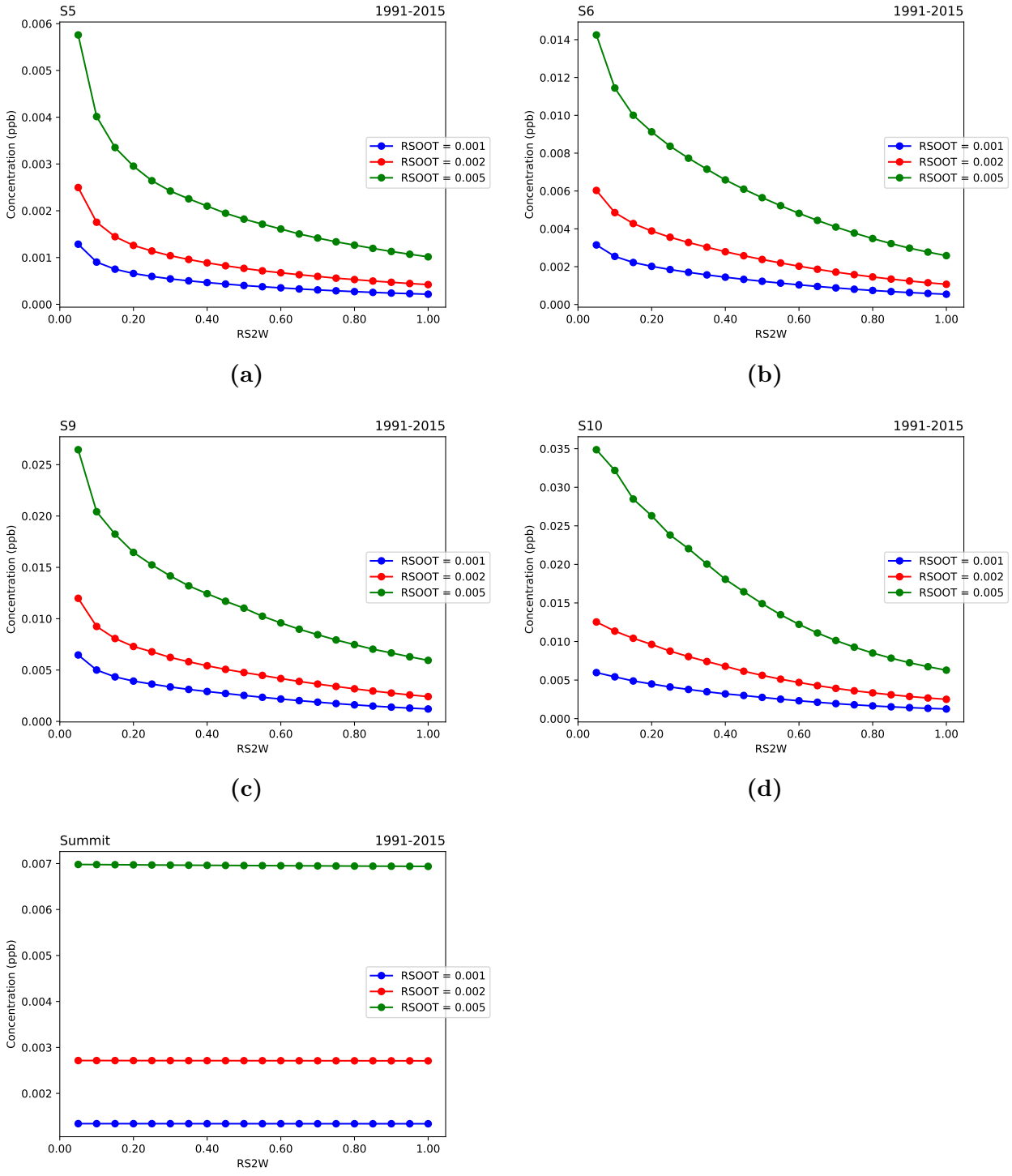

Figure 6: Mean surface soot concentration for the period 1991-2015 during the melt season (1 June until 30 September) for different initial soot concentrations. The subfigures show the situation for the stations a) S5, b) S6, c) S9, d) S10 and e) Summit.

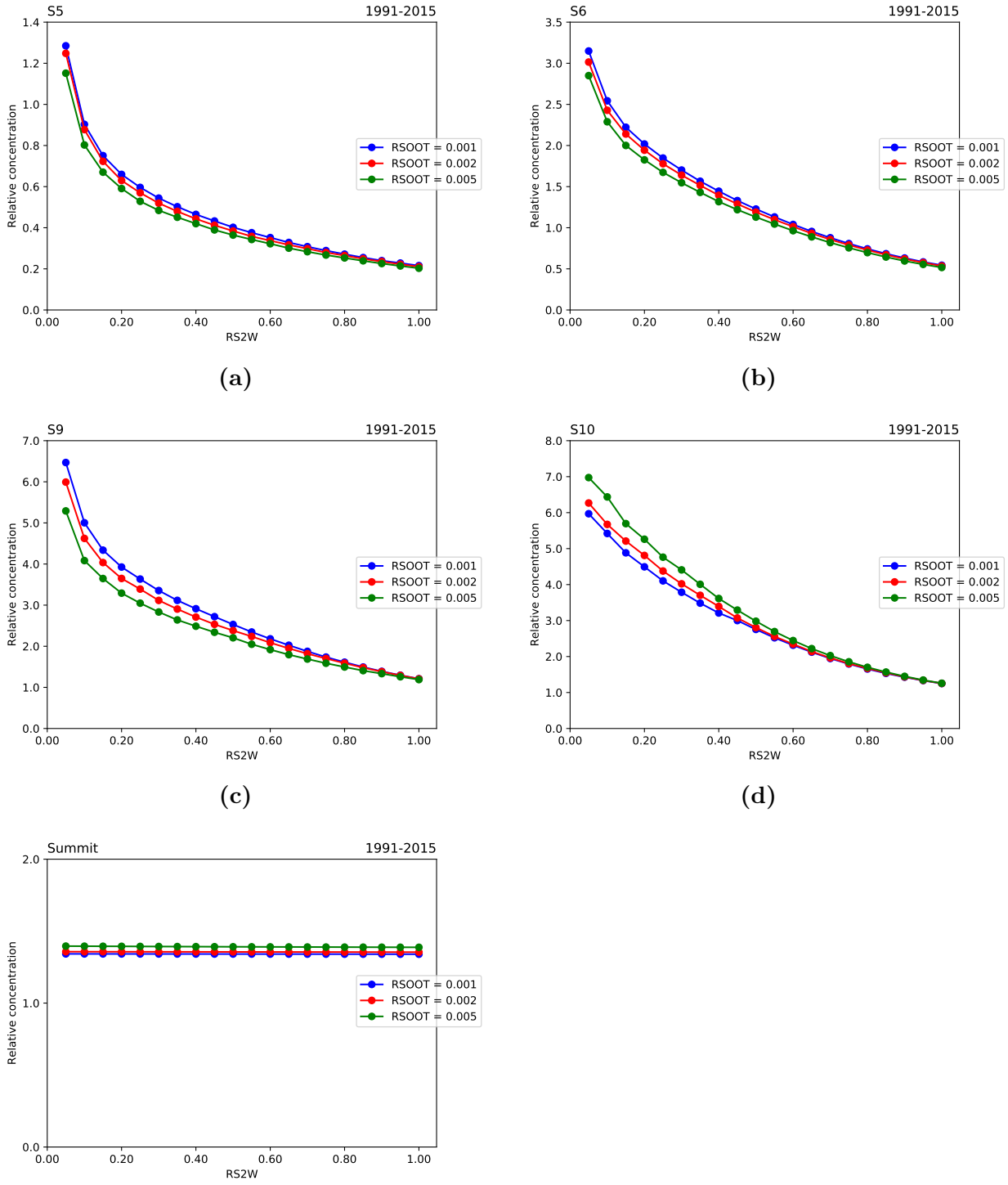

Figure 7: Relative mean surface soot concentration for the period 1991-2015 during the melt season (1 June until 30 September) for different initial soot concentrations. The subfigures show the situation for the stations a) S5, b) S6, c) S9, d) S10 and e) Summit.

soot concentration of 0.001 ppb leads to the lowest mean surface concentration during the melt season as a function of RS2W-value, respectively followed by initial soot concentrations of 0.002 and 0.005 ppb. Increasing RS2W-values lead to a lower mean surface soot concentration, but this effect is not linear.

The mean surface soot concentration is independent of the RS2W-value at station Summit. This is caused by the very limited melt at this location. Due do this very limited melt no meltwater is available to percolate into the firn layer and therefore the surface soot concentration cannot increase. Due to the absence of meltwater a changing RS2W-value has no effect on the mean surface soot concentration.

Figure 7 shows the division of the mean surface soot concentration by the initial soot concentration. This figure makes clear that the relative effects are similar for initial soot concentrations of 0.001, 0.002 and 0.005 ppb. The high relative concentrations at S9 and S10 are remarkable. On these locations the amount of melt is smaller compared to the melt at the stations S5 and S6. This result shows that a larger amount of melt does not lead necessarily to a higher mean surface soot concentration.

4.3 Surface energy balance

The albedo of the firn layer is affected by the soot concentration of the firn. An increasing soot concentration has a negative effect on the upward (reflected) shortwave radiation and albedo and vice versa. This effect makes it possible to use the shortwave radiation and albedo as an indicator to analyze the effect of changing soot concentrations.

Furthermore, AWS data of the down- and upward shortwave radiation fluxes is available. Therefore it is possible to compare both the model output and the AWS data with each other and see for which parameter values the model fits the best to the AWS data.

4.3.1 Static soot distribution

Firstly, we investigate the effects of different initial soot concentrations by using a static soot distribution. One of these concentrations is an initial concentration of 0.050 ppb, which is normally chosen to perform simulations with RACMO2.

Shortwave radiation
Table 2 shows the modelled upward shortwave radiation for simulations with different soot concentrations and the upward shortwave radiation obtained from AWS data. A linear fit with the in situ upward shortwave radiation on the x-axis and the modelled upward shortwave radiation on the y-axis gives more statistical information, including the root-mean-square error (RMSE) and the correlation coefficient (R^2) shown in Table 2.

Table 2 makes clear that R^2 remains almost the same at stations S6, S9 and S10 for different initial soot concentrations. At S6 R^2 increases when the initial soot concentration increases. At S10 R^2 decreases when the soot concentration increases. At S9 R^2 is the highest for an initial soot concentration of 0.010 ppb, from the concentrations for which R^2 is calculated. The changes in the RMSE follow the pattern of R^2, which means the RMSE decreases if R^2 increases and vice versa. Because changes in R^2 are small, it is difficult to

Table 2: Modelled and observed mean upward shortwave radiation and statistics of the differences at S6, S9 and S10. The values are calculated for the period 2003-2015 (S6 and S9) and 2009-2015 (S10). RSOOT is expressed in ppb, the mean, model bias and RMSE are expressed in $\mathrm{W\,m^{-2}}$ and R^2 is dimensionless.

	S6				S9				S10			
RSOOT	mean	bias	RMSE	R^2	mean	bias	RMSE	R^2	mean	bias	RMSE	R^2
OBS	90.7	-	-	-	104.8	-	-	-	121.6	-	-	-
0.000	91.7	0.9	25.1	0.920	111.8	7.0	20.5	0.962	120.2	-1.3	17.9	0.972
0.0005	91.2	0.4	24.7	0.921	111.2	6.4	20.1	0.963	119.8	-1.8	18.0	0.972
0.001	90.9	0.2	24.6	0.922	110.7	5.9	19.7	0.963	119.7	-1.9	18.0	0.972
0.002	90.5	-0.2	24.4	0.922	110.2	5.3	19.2	0.964	119.3	-2.3	18.3	0.972
0.003	90.3	-0.4	24.3	0.922	109.3	4.5	18.5	0.966	119.0	-2.5	18.4	0.972
0.004	90.0	-0.7	24.1	0.923	108.7	3.9	18.2	0.966	118.8	-2.8	18.5	0.972
0.005	89.8	-0.9	24.0	0.923	108.3	3.5	17.9	0.967	118.6	-3.0	18.6	0.971
0.010	88.9	-1.8	23.8	0.924	106.4	1.6	17.3	0.968	117.7	-3.9	19.3	0.970
0.020	87.7	-3.1	23.8	0.923	104.8	-0.1	17.3	0.967	116.7	-4.9	19.7	0.970
0.025	87.2	-3.6	23.7	0.924	104.0	-0.8	17.5	0.967	116.1	-5.5	20.1	0.970
0.050	85.3	-5.4	23.7	0.927	102.1	-2.7	18.1	0.966	114.1	-7.5	22.0	0.967

Table 3: Observed and modelled mean downward shortwave radiaton values at S6, S9 and S10. The values are calculated for the period 2003-2015 (S6 and S9) and the period 2009-2015 (S10). The mean, model bias and RMSE are expressed in $\mathrm{W\,m^{-2}}$ and R^2 is dimensionless.

	S6				S9				S10			
	mean	bias	RMSE	R^2	mean	bias	RMSE	R^2	mean	bias	RMSE	R^2
OBS	127.8	-	-	-	138.9	-	-	-	149.0	-	-	-
RACMO2	137.6	9.8	27.2	0.959	141.7	2.8	22.6	0.970	150.2	1.2	23.1	0.971

base any conclusions on this small differences, although both the RMSE and R^2 follow the same pattern.

The most relevant statistical quantity is the model bias. Table 2 shows that it is possible to reduce the model bias by choosing the appropriate soot concentration. To minimize the bias at S6 a soot concentration between 0.001 ppb and 0.002 ppb is needed. To do the same for S9 a soot concentration of approximately 0.020 ppb is needed. It is not possible to get a bias of 0.0 $\mathrm{W\,m^{-2}}$ for S10 on this way, because the bias is still -1.3 $\mathrm{W\,m^{-2}}$ for a simulation without any soot (0.000 ppb). The decreasing bias for a decreasing soot concentrations suggests that the bias would approach 0.0 $\mathrm{W\,m^{-2}}$ if it would be possible to lower the initial soot concentration even more, which is, of course, physically not possible.

The weather circumstances are the most stable during the year at the location where S10 is situated. Therefore it is most suitable to base conclusions on data of this location. Based on data of S10 a low soot concentration seems to be the best option, which is very different from the initial soot concentration of 0.050 which is oftend used for simulations.

One of the assumptions being made by using this method is that the modelled downward shortwave radiation flux is very similar to the in situ downward shortwave radiation flux. However, Table 3 makes clear that this quantity has also a model bias. The bias in the downward shortwave radiation is 9.8 $\mathrm{W\,m^{-2}}$ at S6, 2.8 $\mathrm{W\,m^{-2}}$ at S9 and 1.2 $\mathrm{W\,m^{-2}}$ at S10. The literature about RACMO2.3p1 mentions a bias of 3.2 $\mathrm{W\,m^{-2}}$ at S9 and 1.8 $\mathrm{W\,m^{-2}}$ at S10. The bias is not calculated for S6 in this paper because of gaps in the AWS data (Noël et al., 2015). The differences between these biases and the biases in Table 2 might be caused by the fact that the biases in the literature are calculated for the period 2004-2012, while data for the period 2003-2015 is used in this thesis.

One of the ways to take the model bias in the downward shortwave radiation into account is by analyzing the albedo instead of the upward shortwave radiation. A bias in the modelled downward shortwave radiation is assumed to lead also to a bias in the upward shortwave radiation. Because the albedo is calculated by dividing the upward shortwave radiation by the downward shortwave radiation, the biases cancel partly away against each other.

Table 4: Observed and modelled mean albedo at S6 and S9. The values are calculated for the period 2003-2015. RSOOT is expressed in ppb, all the statistical quantities are dimensionless.

	S6				S9			
RSOOT	mean	bias	RMSE	R^2	mean	bias	RMSE	R^2
OBS	0.756	-	-	-	0.796	-	-	-
0.000	0.702	-0.054	0.128	0.650	0.812	0.016	0.078	0.565
0.0005	0.699	-0.057	0.128	0.658	0.808	0.012	0.076	0.574
0.001	0.698	-0.058	0.128	0.661	0.805	0.009	0.075	0.557
0.002	0.696	-0.060	0.128	0.666	0.802	0.006	0.073	0.575
0.003	0.695	-0.061	0.128	0.670	0.796	0.000	0.072	0.569
0.004	0.694	-0.063	0.128	0.673	0.792	-0.004	0.071	0.576
0.005	0.692	-0.064	0.128	0.676	0.789	-0.006	0.069	0.598
0.010	0.688	-0.068	0.129	0.685	0.796	-0.018	0.072	0.597
0.020	0.681	-0.075	0.132	0.692	0.769	-0.027	0.076	0.594
0.025	0.678	-0.078	0.133	0.696	0.764	-0.032	0.080	0.581
0.050	0.668	-0.088	0.136	0.710	0.753	-0.042	0.084	0.598

Albedo

Table 4 and 5 show the albedo for different initial soot concentrations including the statistics of a comparison with AWS data. All days for which the modelled or observed daily mean downward shortwave radiation fluxes are smaller than 10.0 $\mathrm{W\,m^{-2}}$ are excluded from the data. This is done because the division amplifies small deviations in the shortwave radiation fluxes. A low downward shortwave radiation flux means also that it is very dark at that location on the GrIS.

For station S6 R^2 increases for increasing initial soot concentrations. For station S9 R^2 seems to increase when the soot concentration increases, although the pattern of R^2 is more irregular. The pattern of R^2 is even more irregular for station S10 according to Table 5,

Table 5: Observed and modelled mean albedo at S10. The values are calculated for the period 2009-2015. RSOOT is expressed in ppb, all the statistical quantities are dimensionless.

	S10			
RSOOT	mean	bias	RMSE	R^2
OBS	0.845	-	-	-
0.000	0.820	-0.025	0.057	0.455
0.0005	0.817	-0.028	0.058	0.457
0.001	0.817	-0.028	0.058	0.470
0.002	0.814	-0.031	0.060	0.460
0.003	0.813	-0.032	0.060	0.458
0.004	0.812	-0.034	0.061	0.456
0.005	0.810	-0.035	0.062	0.452
0.010	0.806	-0.039	0.066	0.448
0.020	0.800	-0.045	0.069	0.460
0.025	0.797	-0.048	0.072	0.458
0.050	0.786	-0.059	0.082	0.459

which makes it not possible to say anything about the relationship between the albedo and the initial soot concentration. At S6 the RMSE increases for increasing soot concentrations. At S9 the RMSE is at a minimum for RSOOT = 0.010 ppb. At S10 the RMSE increases when the initial soot concentration increases. For both S6 and S10 the bias is the smallest for a situation without any soot. At S9 the bias is 0.000 for a soot concentration of 0.003 ppb. These results show again that a low soot concentration seems to be the best option. Figure 8 shows a comparison between the modelled and observed albedo for a static soot concentration of 0.001 ppb. This concentration is chosen because it gives (nearly) an optimal result at both locations. The red line shows a linear fit.

Sensitivity

To determine the importance of knowing the exact soot concentration, the sensitivity of the albedo for different soot concentrations is calculated. Figure 9 shows the albedo as a function of initial soot concentration.

For all locations the albedo decreases when the soot concentration increases. The marginal effect diminishes for increasing initial soot concentrations at all locations. The figure shows also that the effect of an increasing soot concentration is relatively limited at stations S5 and Summit, is stronger at stations S6 and S10 and is the strongest at station S9. Changing the initial soot concentration from 0.050 to 0.001 ppb has a positive effect of 7.3% on the albedo at station S9. These results indicate that the albedo is mainly sensitive to changing soot concentrations along the K-transect and similar regions. The effects at other locations on the GrIS are probably less significant.

4.3.2 Dynamic soot concentration and comparison

Secondly, we investigate the effects of the dynamic soot distribution. The dynamic firn layer model is evaluated using initial soot concentrations of 0.0005, 0.001, 0.002 and 0.005 ppb.

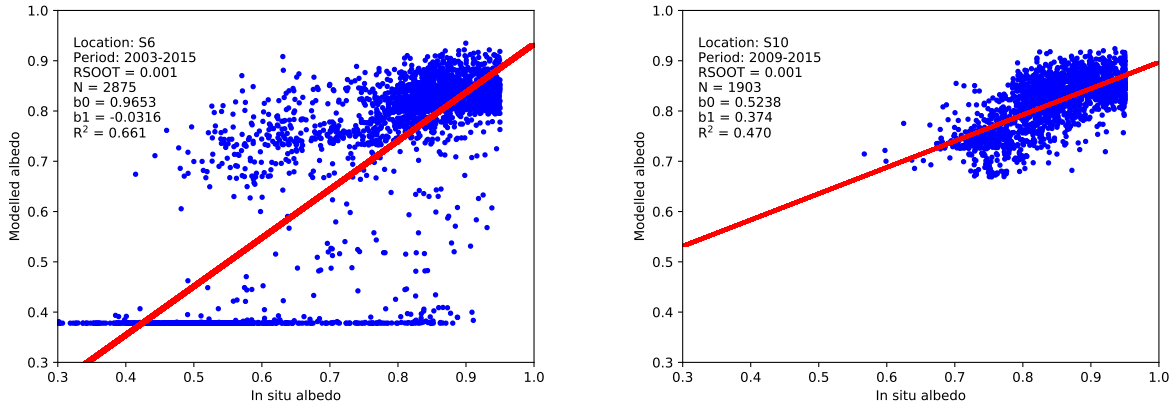

(a) **(b)**

Figure 8: Comparison between the daily average modelled and observed albedo at a) S6 and b) S10. The red line shows the linear fit.

For each initial soot concentration 21 simulations are performed, using 21 different RS2W-values. The simulations were performed for stations S5, S6, S9, S10 and Summit. For S6, S9 and S10 the model output was compared with AWS data. The tables in the appendix show the statistics of the upward shortwave radiation fluxes and albedo for these locations. The most relevant results will be discussed below and compared with the results of the static soot distribution.

Upward shortwave radiation

Table 6 shows the optimal model parameters values for the upward shortwave radiation for the locations S6, S9 and S10, both for the statically and dynamically modelled soot distribution.

For S6 there are two combinations of model parameter values for which the model bias is reduced to W m^{-2}. A minimized bias is achieved for an initial soot concentration of 0.0005 ppb and a RS2W-value between 0.40 and 0.45 and for an initial soot concentration of 0.001 ppb and a RS2W-value between 0.90 and 0.95. The model bias is also minimized using a static initial soot concentration between 0.001 and 0.002 ppb. The correlation coefficients are the same (at least upto three decimals) for all these simulations and the root-mean-square errors are almost the same.

Regarding S9, the model bias is minimized for an initial soot concentration of 0.005 ppb and a RS2W-value of 0.20. The bias is also minimized for a static initial soot concentration between 0.019 and 0.020 ppb. Table 6 shows also that the root-mean-square errors are almost the same in both cases. The correlation coefficients are exactly the same (at least up to three decimals).

Regarding S10, there is no combination of parameters for which the bias in the upward shortwave radiation reduces to 0.0 W m^{-2}. Using the dynamic soot distribution the bias is the smallest for an initial soot concentration of 0.0005 ppb and a RS2W-value of 1.00. The simulation with these parameters is the situation with the lowest soot concentration of

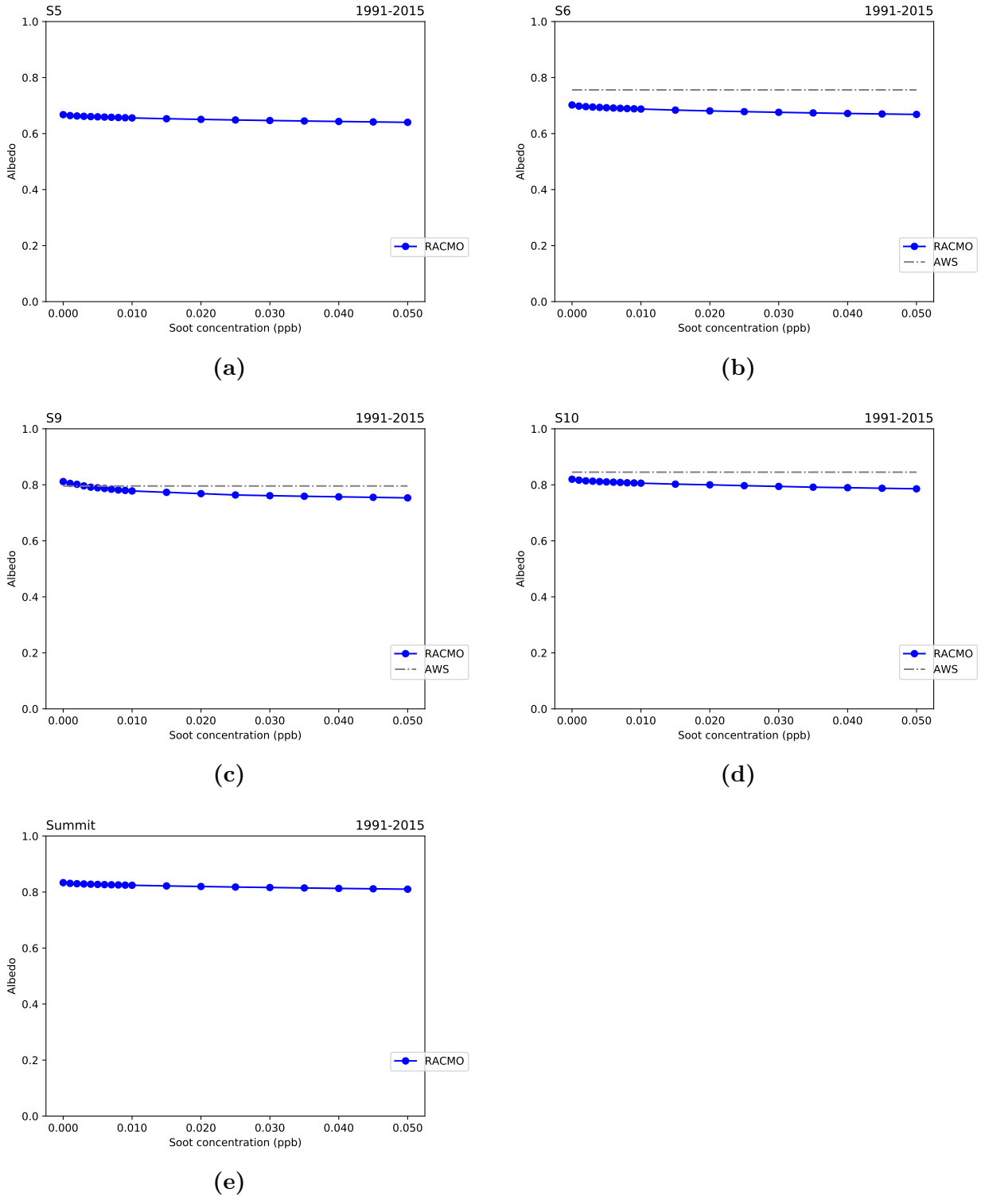

Figure 9: Albedo as a function of soot concentration. The albedo is calculated for a) S5, b) S6, c) S9, d) S10 and e) Summit. For S6, S9 and S10 the albedo obtained from AWS data is shown by a dashed line.

Table 6: Simulations at S6, S9 and S10 for which the bias in the upward shortwave radiation is minimized. RSOOT is expressed in ppb, the mean, model bias and RMSE are expressed in $\mathrm{W\,m^{-2}}$, RS2W and R^2 are dimensionless.

	Settings		Observed	Statistics			
AWS	RSOOT	RS2W	mean	mean	bias	RMSE	R^2
S6	0.001	fixed	90.7	90.9	0.2	24.6	0.922
S6	0.002	fixed	90.7	90.5	-0.2	24.4	0.922
S6	0.0005	0.45	90.7	90.7	-0.0	24.4	0.922
S6	0.0005	0.50	90.7	90.8	0.0	24.4	0.922
S6	0.001	0.90	90.7	90.7	0.0	24.4	0.922
S6	0.001	0.95	90.7	90.8	0.0	24.5	0.922
S9	0.019	fixed	104.8	104.9	0.1	17.3	0.967
S9	0.020	fixed	104.8	104.8	-0.1	17.3	0.967
S9	0.005	0.20	104.8	104.9	0.0	17.4	0.967
S10	0.000	fixed	121.6	120.2	-1.3	17.9	0.972
S10	0.0005	1.00	121.6	119.8	-1.8	18.0	0.972

all simulated dynamic soot distributions. Using the static soot distribution the bias is the smallest if there is no soot at all. No difference emerges between the correlation coefficients and also the root-mean-square errors are almost the same. The model bias is smaller for the static soot distribution than for the dynamic soot distribution (-1.3 $\mathrm{W\,m^{-2}}$ versus -1.8 $\mathrm{W\,m^{-2}}$). This is logical, because the simulation using the static soot distribution was performed with no soot at all.

Albedo

Table 7 shows the optimal model parameter values for the albedo for the locations S6, S9 and S10, both for the static and dynamic soot distribution.

Concerning S6, there is no combination of parameters for which the bias in the albedo reduces to 0.000. Using the dynamic soot distribution the bias is the smallest for an initial soot concentration of 0.0005 ppb and a RS2W-value of 1.00. Using the static soot distribution the bias is the smallest if there is no soot at all. The simulation with these parameters is the situation with the lowest soot concentration of all simulated dynamic situations. The bias is smaller for the static soot distribution (-0.054) than for the dynamic soot distribution (-0.057). The root-mean-square errors are the same in both cases. R^2 is higher for the dynamic than for the static soot distribution (0.659 versus 0.650).

Using the dynamic soot distribution for S9 the model bias is minimized for an initial soot concentration of 0.0005 ppb and a RS2W-value 0.05, an initial soot concentration of 0.001 ppb and a RS2W-value of 0.35 and an initial soot concentration of 0.0020 ppb and a RS2W-value of 0.85. The bias is also minimized for a static soot distribution of 0.003 ppb. The root-mean-square errors are almost the same in these four cases. The differences in the correlation coefficients are larger: R^2 is smaller for the static soot distribution than for the dynamic soot distribution.

Table 7: Simulations at S6, S9 and S10 for which the bias in the albedo is minimized. RSOOT is expressed in ppb, all the other values are dimensionless.

	Settings		Observed	Statistics			
AWS	RSOOT	RS2W	mean	mean	bias	RMSE	R^2
S6	0.000	fixed	0.756	0.702	-0.054	0.128	0.650
S6	0.0005	1.00	0.756	0.699	-0.057	0.128	0.659
S9	0.003	fixed	0.796	0.796	0.000	0.072	0.569
S9	0.0005	0.05	0.796	0.796	0.001	0.071	0.579
S9	0.001	0.35	0.796	0.796	-0.000	0.071	0.575
S9	0.002	0.85	0.796	0.796	-0.000	0.071	0.576
S10	0.000	fixed	0.845	0.820	-0.025	0.057	0.455
S10	0.0005	1.00	0.845	0.817	-0.028	0.058	0.459

Regarding S10, there is no combination for which the bias in the albedo decreases to zero. Using the dynamic soot concentration the bias is the smallest for an initial soot concentration of 0.0005 ppb and a RS2W-value of 1.00. Using the static soot distribution the bias is the smallest if there is no soot at all. The bias is a little smaller for the static soot concentration compared to the dynamic soot distribution (-0.025 compared to -0.028). The root-mean-square errors are almost the same. R^2 is larger for the dynamic soot distribution than for the static soot distribution.

Sensitivity

A changing RS2W-value affects the albedo of the firn, as was already discussed before. The question is still how strongly the albedo reacts on changing RS2W-values. Figure 10 shows the albedo as a function of RS2W-value for five locations. The subfigures for S6, S9 and S10 include an observational average. Figure 10 makes clear that the effect of an increasing RS2W-value is very small at the stations S5 and Summit. The effect becomes larger at S6 and S10 and is the largest at S9. Although the effect is the largest at S9, the effect is still limited. For an initial soot concentration of 0.001 and 0.005 ppb the albedo increases with 2.4% when the RS2W-value increases from 0.00 to 1.00. For an initial soot concentration of 0.002 ppb, the albedo increases with 2.8%.

The subfigures in Figure 11 show the montly mean albedo at stations S5, S6, S9, S10 and Summit. The figures show the montly mean albedo for a static soot concentration of 0.001 and 0.050 ppb. For S6, S9 and S10 the albedo for which the model bias is minimized are also shown. For some months no albedo is included in the figure. This is caused by excluding all days for which the mean downward shortwave radiation is smaller than 10.0 $\mathrm{W\,m^{-2}}$.

Figure 11 makes clear that changing the initial soot concentration from 0.050 to 0.001 ppb has the largest effect. The effect is the largest at station S9. For S5 and S6 the differences emerge only for the first months of the year (until July). The differences between a simulation with a static soot concentration of 0.001 ppb and simulations for which the model bias in the static and dynamic firn layer model is minimized, are very small.

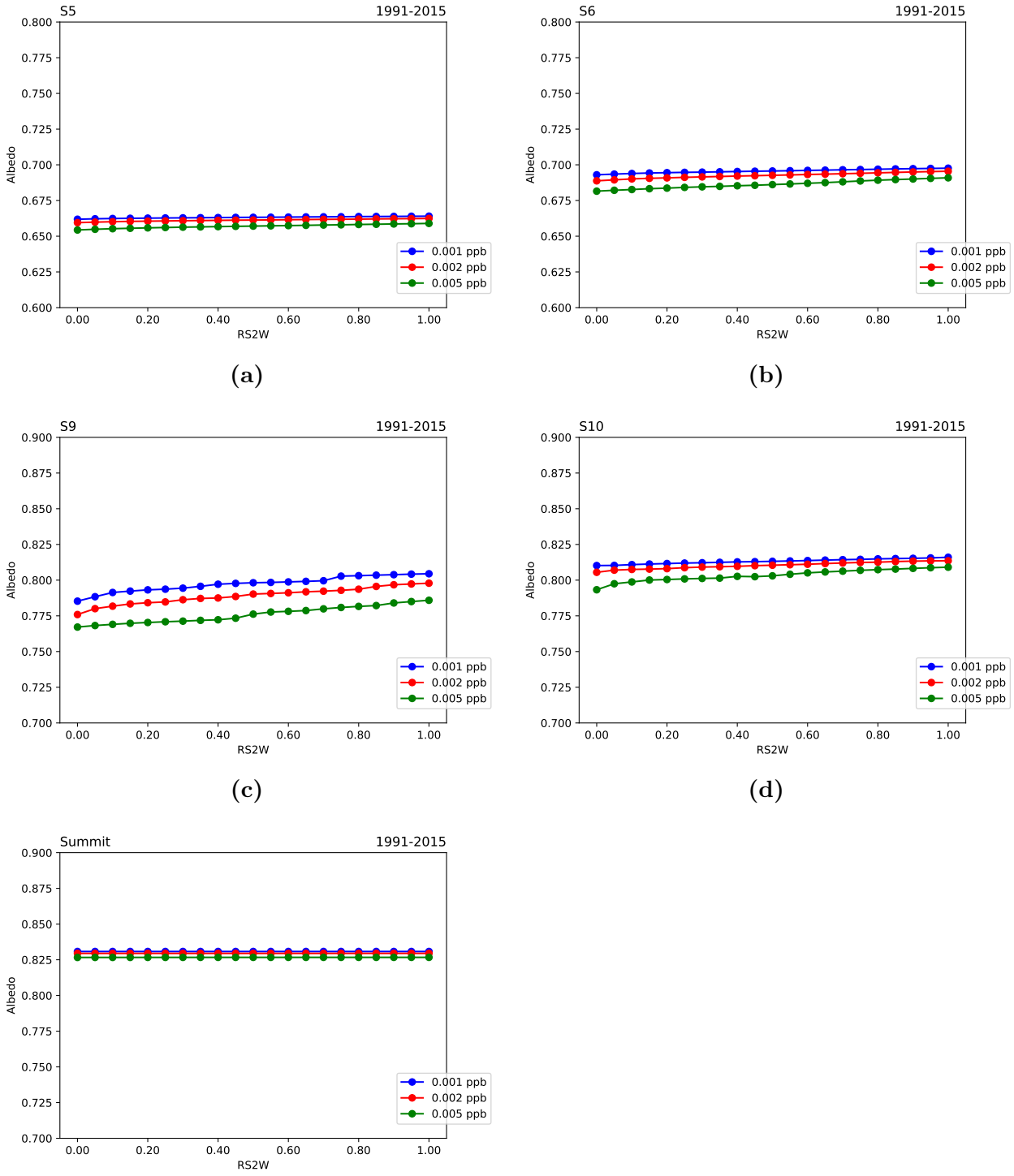

Figure 10: Albedo as a function of RS2W-value for different initial soot concentrations. The albedo is calculated for a) S5, b) S6, c) S9, d) S10 and e) Summit. For S6, S9 and S10 the albedo obtained from AWS data is shown by a dashed line.

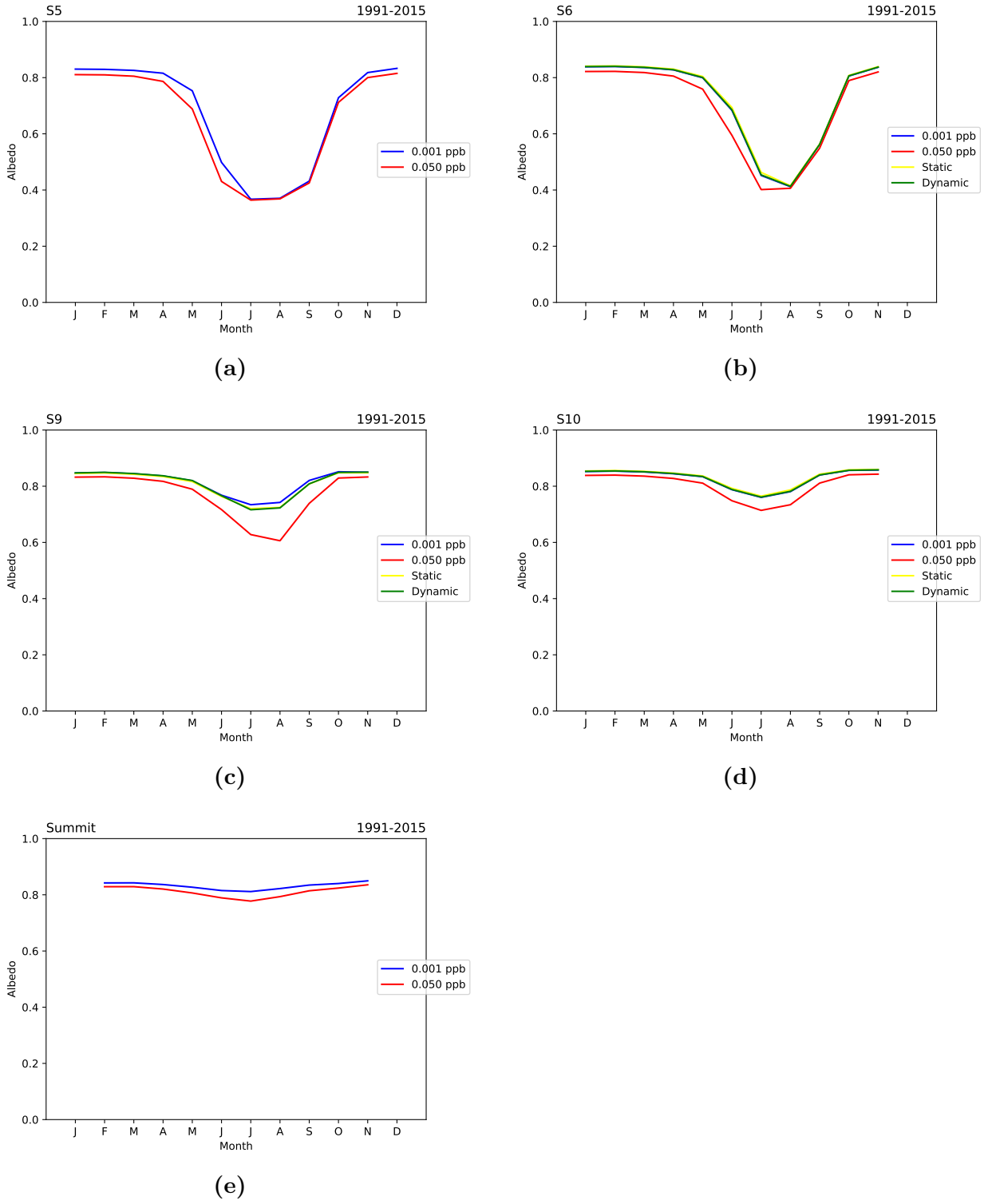

Figure 11: Monthly mean albedo for fixed soot concentrations of 0.001 and 0.050 ppb for a) S5, b) S6, c) S9, d) S10 and e) Summit. For S6, S9 and S10 the monthly mean albedo using the optimal parameter values for both the static and dynamic soot distribution are also shown.

Table 8: SMB of S6 for the period 1991-2015. The table includes the SMB of a static soot concentration of 0.050 ppb (top), the SMB of simulations for which the model bias in the upward shortwave radiation is minimized (middle) and the SMB of simulations for which the model bias in the albedo is minimized (bottom). RSOOT is expressed in ppb, RS2W is dimensionless, the mean and standard deviation are expressed in m w.e.yr^{-1} and the total SMB is expressed in m w.e.

Settings		Statistics		
RSOOT	RS2W	mean	std.	total
0.050	fixed	-2.4	0.6	-59.4
0.001	fixed	-2.0	0.7	-50.3
0.002	fixed	-2.0	0.7	-51.0
0.0005	0.45	-2.0	0.6	-50.8
0.0005	0.50	-2.0	0.6	-50.8
0.001	0.90	-2.0	0.7	-50.8
0.001	0.95	-2.0	0.7	-50.7
0.000	fixed	-2.0	0.7	-48.9
0.0005	1.00	-2.0	0.7	-50.0

4.4 Surface mass balance

A lower albedo enhances snow melting and therefore a changing albedo affects the SMB. This paragraph discusses the SMB for the static and dynamic soot distribution. The paragraph about the SEB made clear that the model bias is minimized for specific model parameter values. The SMB of these simulations are discussed in this paragraph. Table 8, 9 and 10 show the SMB for the stations S6, S9 and S10 respectively. These tables show the SMB of simulations for which the model bias in the upward shortwave radiation or the albedo is minimized. These tables also include the SMB for a simulation with a static soot concentration of 0.050 ppb.

Table 8 shows that all the simulations with optimal parameter values, for both the upward shortwave radiation and the albedo, have a mean SMB of -2.0 m w.e.yr^{-1}. The SMB of a simulation with a static soot concentration of 0.050 ppb gives a mean SMB of -2.4 m w.e.yr^{-1}, which is a difference of -0.4 m w.e.yr^{-1}. Although the annual SMB is equal for all simulations, differences emerge in the SMB for the total period of 25 years. The difference between the smallest and largest value is 2.1 m w.e. during the whole period of 25 years.

Table 9 shows the SMB of simulations for S9. Using the optimal parameter values for the upward shortwave radiation gives a mean SMB of -0.3 m w.e.yr^{-1} and a total effect between -7.5 and -8.1 m w.e. for the total period of 25 years. Using the optimal parameter values for the albedo gives different results. The mean SMB is -0.1 m w.e.yr^{-1} and the total SMB for the period of 25 years varies between -1.5 and -1.8 m w.e. This large difference makes clear that the static and dynamic soot distribution give very different results for the SMB. The SMB of a simulation with a fixed soot concentration of 0.050 ppb gives a mean SMB of -0.5 m w.e.yr^{-1}, which is a difference of -0.2 or -0.4 m w.e.yr^{-1} with respect to the SMB fo simulations using optimal model parameters.

Table 10 shows the SMB for station S10. The optimal model parameters for the upward

Table 9: Same as Table 8 but for station S9.

Settings		Statistics		
RSOOT	RS2W	mean	std.	total
0.050	fixed	-0.5	0.4	-12.4
0.019	fixed	-0.3	0.4	-7.5
0.020	fixed	-0.3	0.4	-7.8
0.005	0.20	-0.3	0.4	-8.1
0.003	fixed	-0.1	0.3	-1.5
0.0005	0.05	-0.1	0.3	-1.8
0.001	0.35	-0.1	0.3	-1.8
0.002	0.85	-0.1	0.3	-1.7

Table 10: Same as Table 8 but for station S10. The optimal values for the model parameters are the same for the upward shortwave radiation and the albedo, so they are only shown once.

Settings		Statistics		
RSOOT	RS2W	mean	std.	total
0.050	fixed	0.3	0.2	7.4
0.000	fixed	0.5	0.1	12.4
0.0005	1.00	0.5	0.1	12.3

shortwave radiation and the albedo are the same. These simulations give a mean SMB of 0.5 m w.e.yr^{-1} and a total SMB of 12.4 m w.e. for the period 1991-2015. The SMB of a simulation with a fixed soot concentration of 0.050 ppb gives a mean SMB of 0.3 m w.e., which is a difference of -0.2 m w.e.yr^{-1} compared to the SMB of the dynamic soot concentration model. The total SMB is 7.4 m w.e. for the period 1991-2015.

Figure 12 shows the annual SMB for S5, S6, S9, S10 and Summit for the period 1991-2015. For all locations the annual SMB for fixed soot concentrations of 0.001 and 0.050 ppb are shown. For S6, S9 and S10 the annual SMB for a static and dynamic soot distribution for which the model parameters are optimal for the albedo (as discussed in the paragraph before), are also shown.

The figure shows that the SMB differences are the largest between simulations with a static soot concentration of 0.001 and 0.050 ppb. The differences between a simulation with a static soot concentration of 0.001 ppb and the simulations for which the albedo is optimal, are very small. Of course this is caused by the fact that the soot concentrations for which the albedo is optimal are in a few cases very near the initial soot concentration of 0.001 ppb. For S6 and S10 it makes no difference for the SMB if a static or dynamic soot concentration is used, using the optimal model parameter values. Most clear differences emerge at S9 for the year 2011.

Figure 13 shows the sensitivity of the SMB as a function of initial soot concentration. The changes are the strongest at S9, smaller at respectively S6, S5 and S10 and the smallest at Summit. The pattern of the soot concentration dependence of the SMB is the same for all locations, although the effects are not equally strong for each locations.

Figure 14 shows the sensitivity of the SMB as a function of RS2W-value. For each location the SMB is calculated for three initial soot concentrations and 21 RS2W-values (0.00 till 1.00 with steps of 0.05). The sensitivity is the largest at S9 and an initial soot concentration of 0.005 ppb gives the largest effect. For a RS2W-value of 0.00 the SMB is -0.4 m w.e.yr^{-1}, but the SMB increases with 0.3 m w.e.yr^{-1} for a RS2W-value of 1.00 (rounded to 1 decimal number). The effects are smaller for lower initial soot concentrations. For an initial soot concentration of 0.001 ppb the SMB increases with 0.2 m w.e.yr^{-1}. For an initial soot concentration of 0.002 ppb, the SMB increases also with 0.2 m w.e.yr^{-1}. At other locations the change in the SMB is smaller for increasing RS2W-values. The subfigures for S5, S6 and S10 show also that the increase of the SMB is smaller when the initial soot concentration is smaller. At station Summit an increasing soot concentration does not change the SMB.

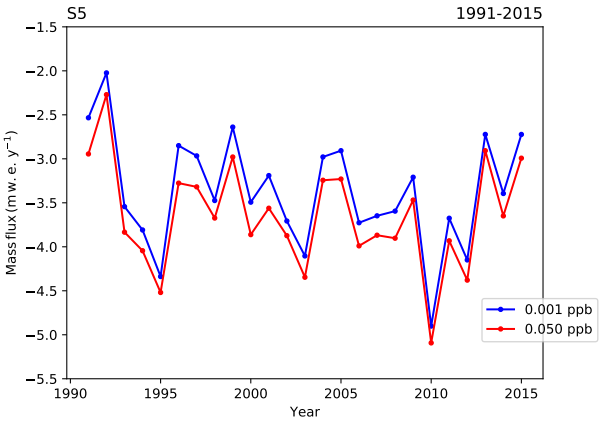

(a)

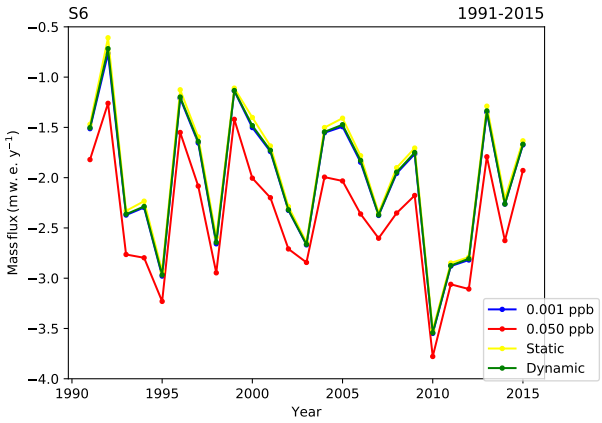

(b)

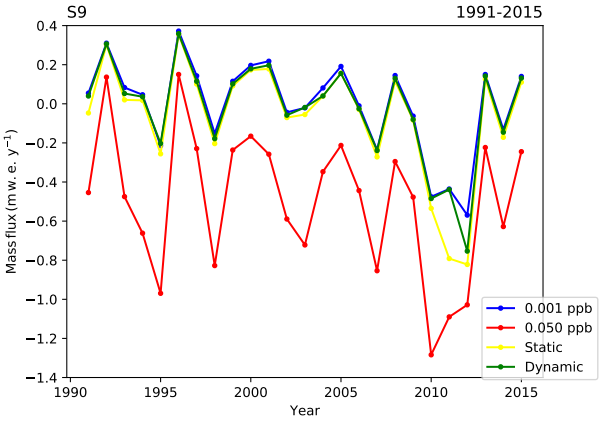

(c)

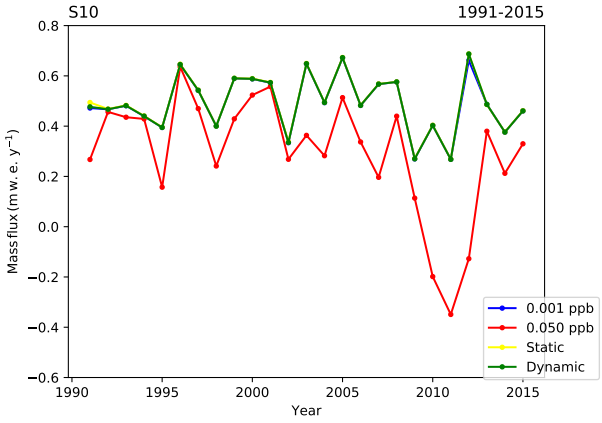

(d)

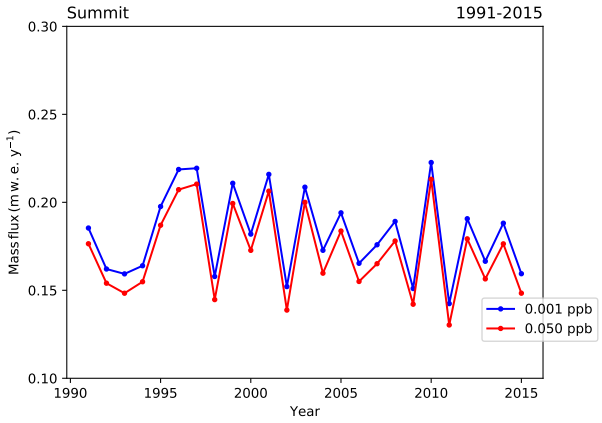

(e)

Figure 12: Annual SMB for a fixed initial soot concentration of 0.001 and 0.050 ppb. For S6, S9 and S10 the SMB obtained by using the optimal parameter values based on the static and dynamic soot distribution are also shown. The SMB is calculated for a) S5, b) S6, c) S9, d) S10 and e) Summit.

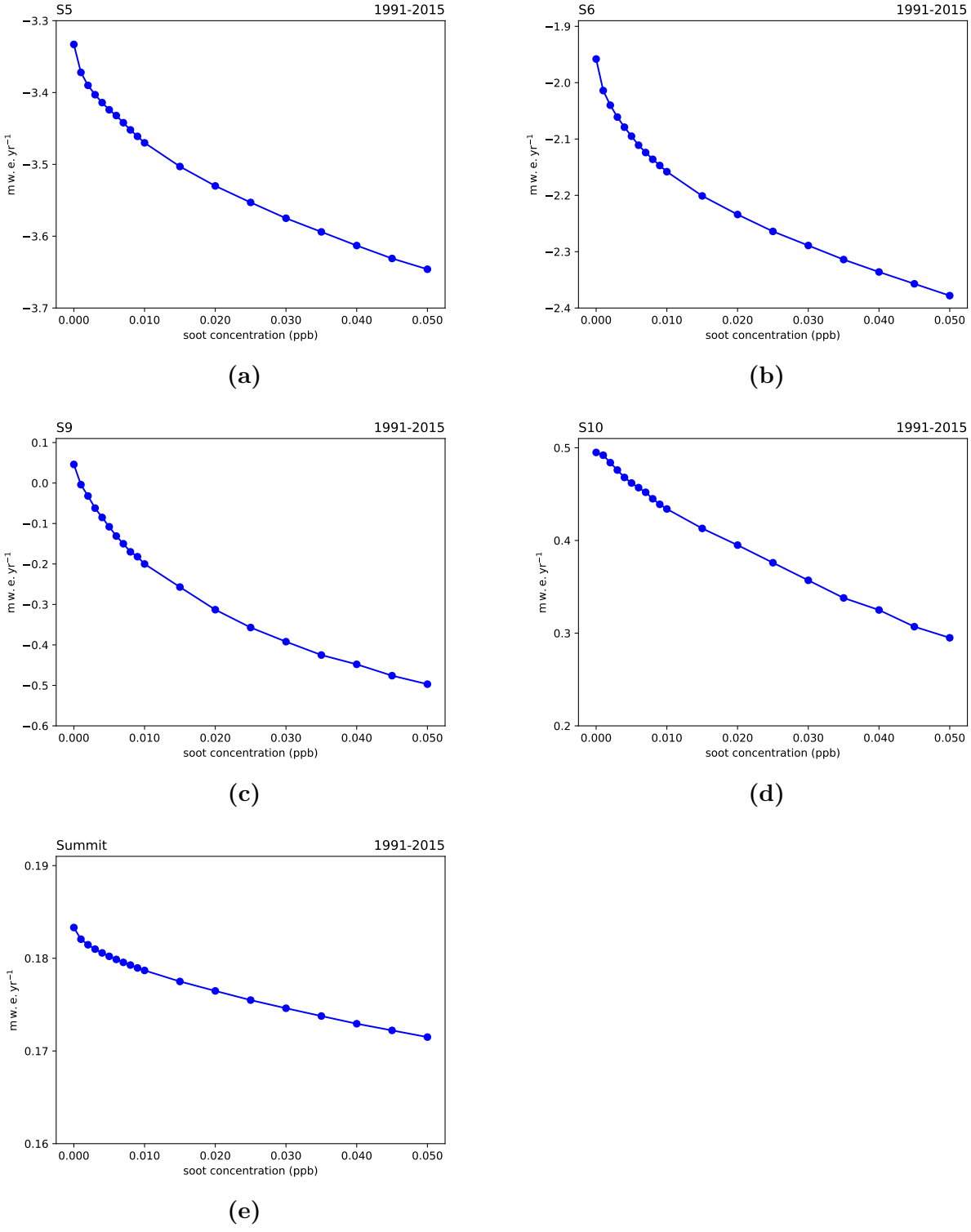

Figure 13: SMB as function of initial soot concentration. Simulations are performed for a) S5, b) S6, c) S9, d) S10 and e) Summit.

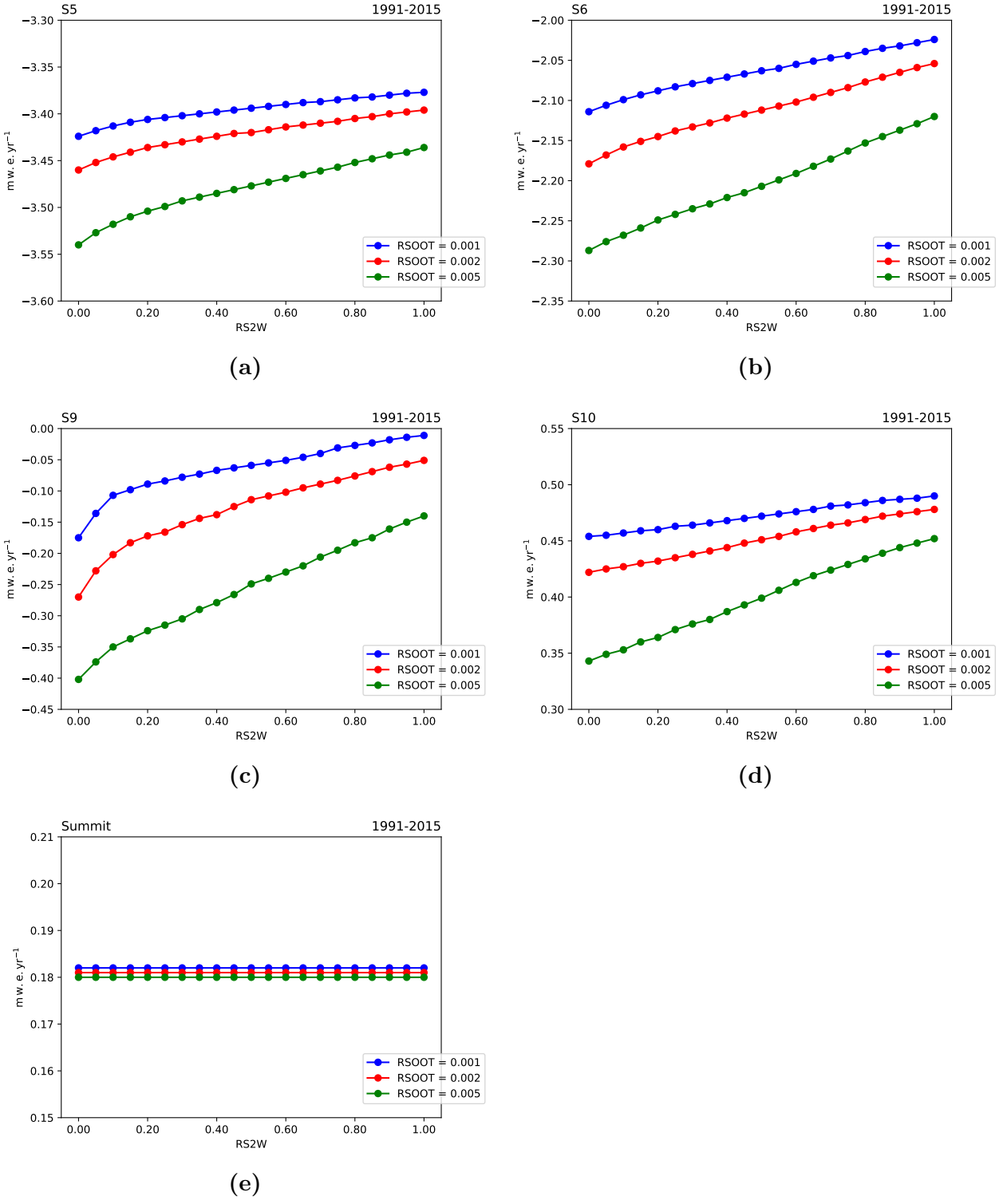

Figure 14: SMB as function of RS2W-value for different initial soot concentrations. Simulations are performed for a) S5, b) S6, c) S9, d) S10 and e) Summit.

5 Discussion

5.1 Firn layer cross sections

The firn layer model of RACMO2.3p2 has been extended with a dynamic description of the soot distribution to improve the modelling of soot in the firn layer. Due to this dynamic soot concentration each model layer has its own soot concentration.

Doherty et al. (2010) analyzed the vertical soot distribution of the firn layer. Simulations for the location where the snow sample was taken give cross sections which are not similar to the observational data. Simulations with a low initial soot concentration give a too low peak value. A higher initial soot concentration gives a better value for the peak concentration, but a too high value for the other levels. It remains challenging to get cross sections which are more similar to the observed cross section.

A simulation for S9 gave a cross section which is more similar to the results obtained by Doherty et al. (2010). This result shows that it is possible to make cross sections like the observed cross section by using the dynamic soot distribution. The problem is, however, that this cross section is based on a simulation for another location and is based on model data of a different date. One of the main differences between these locations is that the melt at S9 is far larger.

It seems that the amount of melt is too low at the location 60 km south of Dye-2 to get such a high concentration as measured by Doherty et al. (2010). If the amount of melt is similar to observational data at this location, another method may be needed to model the distribution of soot on a better way to get cross sections which are more in line with the observations by Doherty et al.

Furthermore, the figure by Doherty et al. (2010) shows precipitation on top of the peak soot concentration, which is not simulated by the model. Therefore the peak concentration in the model is at the surface, instead of a peak in the layer between 10 and 20 cm below the surface.

The soot concentration peak is located within a layer of 10 cm according to Doherty et al. (2010). Most model data show also an increased soot concentration within a layer of this thickness. However, with model layers with a thickness of a few centimeters it is not possible to model the peak concentration in detail. Therefore a smaller thickness of the model layers might be needed to get more detailed cross sections of the firn layer.

A complicating factor in the modelling of the soot concentration is the lack of snow samples, especially snow samples taken along the K-transect. More experimental data is needed to make a good comparison between modelled and observed cross sections.

5.2 Surface soot concentration

The mean surface soot concentration during the melt season is an interesting quantity to analyze the effect of different model parameters on the model output, because the surface soot concentration is directly affected by the dynamic soot distribution. The analysis makes clear that increasing RS2W-values have a negative effect on the mean soot concentration at the surface. A higher initial soot concentration leads to a higher mean surface soot concentration during the melt season. However, the relative effects are equal for different

initial soot concentrations, except for low RS2W-values at S9 and S10.

The absolute effect is different for the five analyzed locations. It is remarkable to see that the effect is far stronger at the stations S9 and S10 and not at S5 and S6, although the melt is larger at these locations. More research is needed to get more insight into the question why the effect is the largest at S9 and S10.

It would be interesting for further research to compare modelled surface soot concentrations with observational concentrations. Because the surface soot concentration is directly affected by the dynamic soot distribution, comparing the surface soot concentration with observational data is a good way to validate te model.

5.3 Surface energy balance (SEB)

Analysis of the SEB of both the static and dynamic soot distribution makes clear that both methods can be used to obtain similar results.

Regarding the upward shortwave radiation, the model bias can be reduced to 0.0 $\mathrm{W\,m^{-2}}$ for S6 and S9 by using the static soot distribution. To reduce the bias to 0.0 $\mathrm{W\,m^{-2}}$ an initial soot concentration between 0.001 and 0.002 ppb is needed for S6 and an initial soot concentration between 0.019 and 0.020 ppb is needed for S9. The model bias is still -1.3 $\mathrm{W\,m^{-2}}$ for a static soot concentration of 0.000 ppb at S10.

The model bias in the upward shortwave radiation can be also reduced to 0.0 $\mathrm{W\,m^{-2}}$ at S6 and S9 by using the dynamic soot distribution. However, the statistics of the differences between model data and AWS data show no better results than the statics of the static soot distribution. At S10 the model bias is the smallest for RSOOT = 0.0005 ppb and RS2W = 1.00. The model bias in the upward shortwave radiation is still -1.8 $\mathrm{W\,m^{-2}}$ for this simulation. This result is not very remarkable, because the firn layer contains more soot in this simulation than in a simulation using a static soot distribution of 0.000 ppb.

Concerning the albedo, it is possible to reduce the bias to 0.000 at S9 by using the static soot distribution with an initial soot concentration of 0.003 ppb. At S6 and S10 the albedo contains still a model bias of respectively -0.054 and -0.025 for a simulation without any soot. At S9 the model bias can also be reduced to 0.000 by using the dynamic soot distribution. For a simulation with RSOOT = 0.0005 ppb and RS2W = 1.00 the model biases in the albedo are -0.057 and -0.028 respectively. Remarkable is the higher R^2 at S9 for the dynamic soot distribution. Also the simulations for S6 and S10 with RSOOT = 0.0005 and RS2W = 1.00 have a higher R^2 compared to the R^2 of the simulation with a static soot concentration of 0.000 ppb. The model bias in the albedo is higher for the static than for the dynamic soot distribution. This result is again not very surprising because the soot concentration is higher for the simulation of the dynamic soot distribution.

The model biases are minized at S6 and S10 for low soot concentrations. Only for the shortwave radiation at S6, the model bias can be reduced to 0.0 $\mathrm{W\,m^{-2}}$. This makes clear that the model bias is also affected by other factors, which are outside the scope of this bachelor project.

At S9 the model biases in the upward shortwave radiation and albedo can be reduced to 0.0 $\mathrm{W\,m^{-2}}$ and 0.000 respectively. However, different parameter values are needed to

minimize the model bias for these quantities. The bias in the upward shortwave radiation is minimized for a static soot concentration between 0.019 and 0.020 ppb, for the albedo the bias is minimized for a static concentration of 0.003 ppb. This concentration difference is quite large. Differences also emerge between the optimal model parameter values based on the upward shortwave radiation and the albedo for the dynamic soot distribution.

There is no combination of parameter values which reduces the bias in the upward shortwave radiation and the albedo for one location to respectively 0.0 $\mathrm{W\,m^{-2}}$ and 0.000. There is also no combination of parameters which reduces the bias in the upward shortwave radiation or the albedo for all locations to respectively 0.0 $\mathrm{W\,m^{-2}}$ or 0.000.

Based on the upward shortwave radiation and albedo, a low soot concentration gives better results than a high soot concentration for most situations. A static soot concentration between 0.000 and 0.002 ppb will give the best results for most locations.

For all locations it is possible to obtain the same results by using the static soot distribution as by using the dynamic soot distribution. The correlation coefficients are a little better for the dynamic soot distribution than for the static soot distribution. Besides this little difference the same results can be achieved using both distributions. This means the added value of the dynamic soot distribution is very limited for the SEB if the simulation is only performed for a seperate location.

However, if locations are analyzed together, or RACMO2 is integrated over the GrIS GrIS, the dynamic soot distribution becomes more relevant. So an important direction for further research is to combine the data for different locations and investigate if the dynamic soot distribution does improve the results for the SEB when more locations are analyzed together.

An analysis of the soot concentration sensitivity of the SEB makes clear that the sensitivity is the largest at S9, is also substantial at S6 and S10 and is the smallest at S5 and Summit. Changing the static soot concentration from 0.050 to 0.001 ppb has a positive effect of 7.3% on the albedo.

The analysis of the sensitivity for different RS2W-values makes clear that the effect of changing RS2W-values on the albedo is far smaller. The effect is again the largest at S9, smaller at S6 and S10 and the smallest at S5 and Summit. From the analyzed initial soot concentrations, the effect is the largest for an initial soot concentration of 0.005 ppb at S9. Changing the RS2W-value from 0.00 to 1.00 leads to an albedo increase of 2.8%.

Although investigating the modelling of soot in firn by analyzing the albedo is interesting because of the availability of AWS data, it remains an indirect way to investigate the effects of changing soot concentrations.

One of the most important limiting factors is the bias in the downward shortwave radiation. This makes the analysis more challenging and the results less reliable. The analysis of the albedo instead of the upward shortwave solves this problem only partly. If the bias in the downward shortwave radiation could be further reduced, the usage of the downward shortwave radiation fluxes and albedo becomes more reliable.

The positive bias in the downward shortwave radiation suggests that the bias in the upward shortwave radiation would also be positive. However, the statistics of the simulation show a negative bias in the upward shortwave radiation for almost all concentrations of S6 and all concentrations of S10. This negative bias in the upward shortwave radiation suggests

that other factors which effect the albedo have to be taken into account. The albedo scheme in the model is based on a paper by Kuipers Munneke et al. (2011). However, recently improvements have been made leading to a better model discription of the albedo scheme (van Dalum, 2020). Using this improved albedo scheme may improve the results described in this thesis.

Also other changes may improve the obtained results. Using data based on RACMO2.3p2 or RACMO2.3p3 (which is currently developed (van Dalum, 2020)) leads to a better simulation of physical processes. Taking into account the radiation penetration might also improve the results.

5.4 Surface mass balance (SMB)

Optimal model parameter values are calculated for the upward shortwave radiation fluxes and albedo. At S6 these simulations all have a SMB of -2.0 m w.e.yr^{-1} (upto one decimal number). It makes no difference if these parameters are based on optimal values based on the shortwave radiation flux or the albedo. It makes also no difference if the static or dynamic soot distribution is used.

However, it is important to consider that the optimal values for the albedo are not based on a situation where the model bias in the albedo is 0.000. It is also important to consider that the optimal model parameter values based on the upward shortwave radiation and the albedo are very close to each other. Therefore the similar SMB is not very surprising. Although the different simulations have the same SMB, differences will emerge if more decimal numbers are taken into account, because they emerge already in the SMB for the period of 25 years.

Concerning S9, simulations with optimal parameter values based on the upward shortwave radiation have the same SMB and simulations based on optimal albedo values have the same SMB. However, the SMB of these two categories of simulations are not equal to each other. The difference in the annual SMB of -0.2 m w.e.yr^{-1} causes large effects on the long term.

Concerning S10, the optimal values for the upward shortwave radiation and the albedo are the same. The values are based on simulations for which the bias is the smallest but is not reduced to 0.0 W m^{-2} or 0.000.

Analysis of the sensitivity makes clear that changing soot concentrations have a larger effect on the SMB than changing RS2W-values. The effects are the largest for locations along the K-transect. From the analyzed locations the effect is the largest for S9. The sensitivity of the SMB of the soot concentration is of the order size of 0.5 m w.e.yr^{-1} for locations along the K-transect and probably also for similar regions. The actual SMB effect is dependent of the initial soot concentration and the exact location.

Different combinations of model parameter values give the same upward shortwave radiation flux or albedo, but have different values for the SMB. Especially at S9 the differences are large. AWS data can show which combination of parameters is the best for the SMB. Therefore it is important to take this data into account in further research.

The obtained optimal parameter values are still suboptimal for S6 and S10, which means the modelled upward shortwave radiation and albedo still have a model bias. These biases have also a different value, which indicates that the optimal parameter values (with no bias)

would be different from each other if the model bias could be completely reduced. So if the model bias could be completely reduced, the optimal model parameter values will probably differ more.

S9 is the location which shows the largest sensitivity for a changing soot concentration, both for the SEB and SMB. The weather circumstances at station S9 are challenging to model. More research is needed to get a better insight in the physical processes at this location. Because the sensitivity is large at this location, it is important to choose the right soot concentration for this location. It might be an idea to use another (fixed) location for S9 than for other locations.

6 Conclusion

The objective of this thesis was to investigate the effects of dynamically modelled impurity concentrations in firn on the GrIS.

It remains challenging to get model cross sections which are similar to the cross section obtained by Doherty et al. (2010). The dynamic soot concentration model itself is able to give results in line with the observationals results, but probably model improvements are needed to get these cross sections for the desired date and location.

The mean surface soot concentration increases during the melt season when the dynamic soot distribution is used. The relative effects are different for different locations, but almost independent of the initial soot concentration. The effect is the largest at S9 and S10 and not at S5 and S6, although the melt is larger at these locations.

Analysis of the SEB makes clear that optimal results for the upward shortwave radiation and albedo can be obtained by using both a statically and dynamically modelled soot concentration, but these optimal results are obtained for different model parameter values. Overall, a static soot concentration between 0.000 and 0.002 ppb seems to give the best results. The dynamic soot distribution does not give a parameter combination which is optimal for both quantities at one location or for one quantity at all locations. Analysis of the sensitivity makes clear that the SEB and SMB are more sensitive to changing soot concentrations than to changing soot removal rates.

Optimal parameter values based on the upward shortwave radiation flux and albedo have different effects on the SMB at S9. At S6 and S10 the effects are more similar, although the used model parameter values are still suboptimal. The SMB is more sensitive to changing soot concentrations than to changing soot removal rates. The order size of the sensitivity is 0.5 m w.e.yr^{-1} for locations along the K-transect.

A References

Box, J. E., Fettweis, X., Stroeve, J. C., Tedesco, M., Hall, D. K., and Steffen K.,: Greenland ice sheet albedo feedback: thermodynamics and atmospheric drivers, The Cryosphere, 6, 812-839, doi:10.5194/tc-6-821-2012, 2012.

Doherty, S. J., Warren, S. G., Grenfell, T. C., Clarke, A. D., and Brandt, R.E.: Light-absorbing impurities in Arctic snow, Atmos. Chem. Phys, 10, 11647-11768,

doi.org/10.5194/acp-10-11647-2010, 2010.

Ettema, J., van den Broeke, M. R., van Meijgaard, E., van de Berg, W. J., Bamber, J. L., Box, J. E., and Bales, C. B.: Higher surface mass balance of the Greenland ice sheet revealed by high-resolution climate modeling, Geophys. Res. Lett., 36(L12501), doi.org/10.1029/2009GL038110, 2009.

Kuipers Munneke, P., van den Broeke, M. R., Lenaerts, J. T. M., Flanner, M. G., Gardner, A. S., and van de Berg, W. J.: A new albedo parameterization for use in climate models over the Antarctic ice sheet, J. Geophys. Res., 116(D05114), doi:10.1029/2010JD015113, 2011.

Kuipers Munneke, P., Ligtenberg, S. R. M., van den Broeke, M. R., van Angelen, J.H., and Forster, R. R.: Explaining the presence of perennial liquid water bodies in the firn of the Greenland Ice Sheet, Geoph. Res. Lett., 41, 476-483, doi:10.1002/2013GL058389, 2014.

Kuipers Munneke, P., Smeets, C. J. P. P., Reijmer, C. H., Oerlemans, J., van de Wal, R. S. W., and van den Broeke, M. R.: The K-transect on the western Greenland Ice Sheet: Surface energy balance (2003-2016), ARctic, Antarctic, and Alpine Research, 50:1, S100003, doi.org/10.1080/15230430.2017.1420952, 2018.

Noël, B., van de Berg, W. J., van Meijgaard, E., Kuipers Munneke, P., van de Wal, R. S. W., and van den Broeke, M. R.: Evaluation of the updated regional climate model RACMO2.3: summer snowfall impact on the Greenland Ice Sheet, The Cryosphere, 9, 1831-1844, doi.org/10.5194/tc-9-1831-2015, 2015.

Noël, B., van de Berg, W. J., van Wessem, J. M., van Meijgaard, E., van As, D., Lenaerts, J. T. M., Lhermitte, S., Kuipers Munneke, P., Smeets, C.J.P., van Ulft, L. H., van de Wal, R. S. W., and van den Broeke, M. R.: Modelling the climate and surface mass balance of polar ice sheets using RACMO2 - Part 1: Greenland (1958-2016), The Cryosphere, 12, 811-831, doi.org/10.5194/tc-12-811-2018, 2018.

Shepherd, A., Ivins, E., Rignot, E. et al.: Mass balance of the Greenland Ice Sheet from 1992 to 2018, Nature, 579, 233-239, doi.org/10.1038/s41586-019-1855-2, 2020.

van Dalum, C. T., van de Berg, W. J., Lhermitte, S., and van den Broeke, M. R.: Evaluation of a new snow albedo scheme for the Greenland ice sheet in the regional climate model RACMO2, The Cryosphere Discuss., doi.org/10.5194/tc-2020-118, in review, 2020.

B Appendix

B.1 Upward shortwave radiation

B.1.1 S6

Table 11: Upward shortwave radiation at S6 for initial soot concentrations of 0.0005 and 0.001 ppb compared to model data for the period 2003-2015. The mean, bias and RMSE are expressed in $\mathrm{W\,m^{-2}}$, RS2W and R^2 are dimensionless.

	RSOOT = 0.0005 ppb				RSOOT = 0.001 ppb			
RS2W	mean	bias	RMSE	R^2	mean	bias	RMSE	R^2
OBS	90.7	-	-	-	90.7	-	-	-
0.00	90.3	-0.4	24.1	0.924	89.7	-1.0	23.8	0.925
0.05	90.4	-0.3	24.1	0.923	89.8	-0.9	23.8	0.925
0.10	90.5	-0.2	24.2	0.923	89.9	-0.8	23.8	0.925
0.15	90.5	-0.2	24.2	0.923	90.0	-0.7	23.9	0.924
0.20	90.6	-0.2	24.3	0.923	90.1	-0.7	23.9	0.924
0.25	90.6	-0.1	24.3	0.923	90.1	-0.6	23.9	0.924
0.30	90.6	-0.2	24.3	0.923	90.2	-0.6	24.0	0.924
0.35	90.7	-0.1	24.3	0.922	90.2	-0.5	24.0	0.924
0.40	90.7	-0.0	24.4	0.922	90.3	-0.5	24.0	0.924
0.45	90.7	0.0	24.4	0.922	90.3	-0.4	24.1	0.923
0.50	90.8	0.0	24.4	0.922	90.3	-0.4	24.1	0.923
0.55	90.8	0.1	24.4	0.922	90.4	-0.3	24.2	0.923
0.60	90.8	0.1	24.4	0.922	90.4	-0.3	24.2	0.923
0.65	90.8	0.1	24.5	0.922	90.5	-0.2	24.3	0.923
0.70	90.9	0.2	24.5	0.922	90.5	-0.2	24.3	0.922
0.75	90.9	0.2	24.5	0.922	90.6	-0.1	24.3	0.922
0.80	90.9	0.2	24.5	0.922	90.6	-0.1	24.4	0.922
0.85	91.0	0.3	24.6	0.922	90.7	-0.0	24.4	0.922
0.90	91.0	0.3	24.6	0.921	90.7	-0.0	24.4	0.922
0.95	91.0	0.3	24.6	0.921	90.8	0.0	24.5	0.922
1.00	91.1	0.3	24.6	0.921	90.8	0.1	24.5	0.922

Table 12: Upward shortwave radiation at S6 for initial soot concentrations of 0.002 and 0.005 ppb compared to model data for the period 2003-2015. The mean, bias and RMSE are expressed in $\mathrm{W\,m^{-2}}$, RS2W and R^2 are dimensionless.

	RSOOT = 0.002 ppb				RSOOT = 0.005 ppb			
RS2W	mean	bias	RMSE	R^2	mean	bias	RMSE	R^2
OBS	90.7	-	-	-	90.7	-	-	-
0.00	88.8	-1.9	23.8	0.923	87.3	-3.4	23.7	0.924
0.05	89.0	-1.7	23.8	0.924	87.4	-3.3	23.6	0.925
0.10	89.1	-1.6	23.8	0.924	87.6	-3.2	23.6	0.925
0.15	89.2	-1.5	23.7	0.924	87.7	-3.0	23.6	0.925
0.20	89.3	-1.4	23.7	0.925	87.8	-2.9	23.7	0.924
0.25	89.4	-1.3	23.7	0.925	87.9	-2.8	23.7	0.924
0.30	89.5	-1.3	23.7	0.925	88.0	-2.7	23.7	0.924
0.35	89.5	-1.2	23.7	0.925	88.1	-2.6	23.8	0.924
0.40	89.6	-1.1	23.7	0.925	88.2	-2.5	23.8	0.923
0.45	89.7	-1.1	23.8	0.925	88.3	-2.4	23.8	0.923
0.50	89.7	-1.0	23.8	0.924	88.4	-2.3	23.8	0.923
0.55	89.8	-0.9	23.8	0.924	88.5	-2.2	23.8	0.924
0.60	89.8	-0.9	23.9	0.924	88.6	-2.1	23.8	0.924
0.65	89.9	-0.8	23.9	0.924	88.7	-2.0	23.8	0.924
0.70	90.0	-0.7	23.9	0.924	88.8	-1.9	23.7	0.924
0.75	90.0	-0.7	24.0	0.924	89.0	-1.8	23.7	0.925
0.80	90.1	-0.6	24.1	0.923	89.1	-1.6	23.7	0.925
0.85	90.2	-0.5	24.2	0.923	89.2	-1.5	23.7	0.924
0.90	90.3	-0.5	24.2	0.922	89.3	-1.4	23.8	0.924
0.95	90.3	-0.4	24.3	0.922	89.4	-1.3	23.8	0.924
1.00	90.4	-0.3	24.3	0.922	89.5	-1.2	23.8	0.924

B.1.2 S9

Table 13: Upward shortwave radiation at S9 for initial soot concentrations of 0.0005 and 0.001 ppb compared to model data for the period 2003-2015. The mean, bias and RMSE are expressed in $\mathrm{W\,m^{-2}}$, RS2W and R^2 are dimensionless.

	RSOOT = 0.0005 ppb				RSOOT = 0.001 ppb			
RS2W	mean	bias	RMSE	R^2	mean	bias	RMSE	R^2
OBS	104.8	-	-	-	104.8	-	-	-
0.00	108.6	3.8	17.9	0.967	107.5	2.7	17.4	0.968
0.05	109.3	4.5	18.4	0.966	108.0	3.2	17.6	0.968
0.10	109.7	4.8	18.8	0.965	108.5	3.7	17.9	0.967
0.15	109.8	5.0	19.0	0.965	108.7	3.9	18.1	0.966
0.20	109.9	5.1	19.2	0.964	108.9	4.0	18.3	0.966
0.25	110.0	5.2	19.2	0.964	109.0	4.1	18.3	0.966
0.30	109.9	5.1	19.2	0.964	109.1	4.2	18.4	0.966
0.35	110.4	5.6	19.5	0.963	109.2	4.4	18.5	0.966
0.40	110.5	5.7	19.5	0.963	109.4	4.6	18.6	0.966
0.45	110.6	5.7	19.5	0.963	109.5	4.7	18.6	0.966
0.50	110.6	5.8	19.6	0.964	109.6	4.8	18.7	0.965
0.55	110.7	5.8	19.6	0.963	109.6	4.8	18.9	0.965
0.60	110.7	5.9	19.6	0.963	109.7	4.9	19.0	0.964
0.65	110.8	5.9	19.7	0.963	109.8	5.0	19.1	0.964
0.70	110.8	6.0	19.8	0.963	109.9	5.0	19.2	0.964
0.75	110.8	6.0	19.8	0.963	110.3	5.4	19.3	0.964
0.80	110.9	6.0	19.9	0.963	110.3	5.5	19.4	0.964
0.85	111.1	6.2	19.9	0.963	110.4	5.6	19.5	0.963
0.90	111.1	6.3	19.9	0.963	110.5	5.7	19.5	0.963
0.95	111.2	6.3	20.0	0.963	110.6	5.7	19.5	0.963
1.00	111.2	6.3	20.0	0.963	110.6	5.8	19.6	0.963

Table 14: Upward shortwave radiation at S9 for initial soot concentrations of 0.002 and 0.005 ppb compared to model data for the period 2003-2015. The mean, bias and RMSE are expressed in $\mathrm{W\,m^{-2}}$, RS2W and R^2 are dimensionless.

	RSOOT = 0.002 ppb				RSOOT = 0.005 ppb			
RS2W	mean	bias	RMSE	R^2	mean	bias	RMSE	R^2
OBS	104.8	-	-	-	104.8	-	-	-
0.00	105.9	1.1	17.4	0.967	104.2	-0.7	17.7	0.966
0.05	106.5	1.7	17.3	0.968	104.4	-0.4	17.5	0.966
0.10	106.8	2.0	17.3	0.968	104.6	-0.2	17.4	0.967
0.15	107.1	2.3	17.4	0.968	104.8	-0.1	17.4	0.967
0.20	107.3	2.4	17.4	0.968	104.9	0.0	17.4	0.967
0.25	107.4	2.5	17.5	0.967	105.0	0.1	17.4	0.967
0.30	107.6	2.8	17.6	0.967	105.1	0.2	17.4	0.967
0.35	107.8	3.0	17.5	0.968	105.2	0.4	17.4	0.967
0.40	107.9	3.0	17.5	0.968	105.3	0.5	17.4	0.967
0.45	108.0	3.2	17.7	0.967	105.5	0.6	17.4	0.967
0.50	108.3	3.5	17.8	0.967	105.9	1.1	17.2	0.968
0.55	108.4	3.6	17.9	0.967	106.1	1.3	17.3	0.968
0.60	108.5	3.7	18.1	0.966	106.2	1.4	17.3	0.967
0.65	108.7	3.8	18.2	0.966	106.3	1.5	17.3	0.967
0.70	108.8	3.9	18.2	0.966	106.6	1.7	17.2	0.968
0.75	108.9	4.0	18.3	0.966	106.7	1.9	17.2	0.968
0.80	109.0	4.2	18.4	0.966	106.9	2.1	17.3	0.968
0.85	109.2	4.4	18.5	0.966	107.0	2.2	17.4	0.967
0.90	109.4	4.6	18.6	0.966	107.3	2.5	17.4	0.968
0.95	109.5	4.7	18.7	0.965	107.5	2.7	17.4	0.968
1.00	109.6	4.8	18.9	0.964	107.7	2.8	17.6	0.967

B.1.3 S10

Table 15: Upward shortwave radiation at S10 for initial soot concentrations of 0.0005 and 0.001 ppb compared to model data for the period 2009-2015. The mean, bias and RMSE are expressed in $\mathrm{W\,m^{-2}}$, RS2W and R^2 are dimensionless.

	RSOOT = 0.0005 ppb				RSOOT = 0.001 ppb			
RS2W	mean	bias	RMSE	R^2	mean	bias	RMSE	R^2
OBS	121.6	-	-	-	121.6	-	-	-
0.00	119.1	-2.4	18.4	0.972	118.5	-3.0	18.6	0.971
0.05	119.1	-2.4	18.4	0.972	118.6	-3.0	18.6	0.971
0.10	119.2	-2.4	18.3	0.972	118.6	-2.9	18.6	0.971
0.15	119.2	-2.4	18.3	0.972	118.7	-2.9	18.6	0.971
0.20	119.2	-2.3	18.3	0.972	118.8	-2.8	18.5	0.971
0.25	119.3	-2.3	18.3	0.972	118.8	-2.7	18.5	0.971
0.30	119.2	-2.3	18.3	0.972	118.9	-2.7	18.5	0.971
0.35	119.4	-2.2	18.2	0.972	118.9	-2.7	18.5	0.971
0.40	119.4	-2.2	18.2	0.972	119.0	-2.6	18.5	0.971
0.45	119.4	-2.1	18.2	0.972	119.0	-2.6	18.4	0.972
0.50	119.5	-2.1	18.1	0.972	119.0	-2.5	18.4	0.972
0.55	119.5	-2.1	18.1	0.972	119.1	-2.5	18.4	0.972
0.60	119.6	-2.0	18.1	0.972	119.1	-2.4	18.4	0.972
0.65	119.6	-1.9	18.1	0.972	119.2	-2.4	18.3	0.972
0.70	119.7	-1.9	18.1	0.972	119.2	-2.3	18.3	0.972
0.75	119.7	-1.9	18.1	0.972	119.3	-2.3	18.3	0.972
0.80	119.7	-1.9	18.1	0.972	119.3	-2.2	18.2	0.972
0.85	119.7	-1.8	18.1	0.972	119.4	-2.2	18.2	0.972
0.90	119.7	-1.8	18.1	0.972	119.4	-2.1	18.2	0.972
0.95	119.7	-1.8	18.1	0.972	119.5	-2.1	18.1	0.972
1.00	119.8	-1.8	18.0	0.972	119.5	-2.0	18.1	0.972

Table 16: Upward shortwave radiation at S10 for initial soot concentrations of 0.002 and 0.005 ppb compared to model data for the period 2009-2015. The mean, bias and RMSE are expressed in $\mathrm{W\,m^{-2}}$, RS2W and R^2 are dimensionless.

	RSOOT = 0.002 ppb				RSOOT = 0.005 ppb			
RS2W	mean	bias	RMSE	R^2	mean	bias	RMSE	R^2
OBS	121.6	-	-	-	121.6	-	-	-
0.00	117.7	-3.9	19.2	0.970	115.3	-6.3	21.7	0.965
0.05	117.9	-3.7	19.0	0.971	115.9	-5.7	21.0	0.967
0.10	118.0	-3.6	19.0	0.971	116.1	-5.4	20.8	0.967
0.15	118.0	-3.5	19.0	0.971	116.3	-5.2	20.7	0.968
0.20	118.1	-3.5	18.9	0.971	116.4	-5.2	20.6	0.968
0.25	118.2	-3.4	18.8	0.971	116.5	-5.1	20.5	0.968
0.30	118.3	-3.3	18.8	0.971	116.6	-5.0	20.4	0.968
0.35	118.3	-3.2	18.7	0.971	116.7	-4.9	20.3	0.968
0.40	118.4	-3.2	18.7	0.971	116.8	-4.7	20.2	0.968
0.45	118.4	-3.1	18.6	0.972	116.8	-4.7	20.2	0.969
0.50	118.5	-3.1	18.6	0.971	117.0	-4.6	20.0	0.969
0.55	118.6	-3.0	18.6	0.971	117.2	-4.4	19.8	0.969
0.60	118.6	-2.9	18.6	0.971	117.4	-4.2	19.7	0.969
0.65	118.7	-2.8	18.6	0.971	117.5	-4.1	19.6	0.970
0.70	118.8	-2.8	18.5	0.972	117.6	-4.0	19.5	0.970
0.75	118.9	-2.7	18.5	0.972	117.7	-3.8	19.4	0.970
0.80	118.9	-2.6	18.5	0.972	117.8	-3.7	19.3	0.970
0.85	119.0	-2.6	18.4	0.972	117.9	-3.7	19.3	0.970
0.90	119.1	-2.5	18.4	0.972	118.0	-3.5	19.2	0.970
0.95	119.1	-2.5	18.4	0.972	118.1	-3.4	19.0	0.971
1.00	119.1	-2.5	18.4	0.972	118.2	-3.3	18.9	0.971

B.2 Albedo

B.2.1 S6

Table 17: Albedo at S6 for initial soot concentrations of 0.0005 and 0.001 ppb compared to model data for the period 2003-2015. RS2W and all statistical quantities are dimensionless.

	RSOOT = 0.0005 ppb				RSOOT = 0.001 ppb			
RS2W	mean	bias	RMSE	R^2	mean	bias	RMSE	R^2
OBS	0.756	-	-	-	0.756	-	-	-
0.00	0.696	-0.060	0.127	0.676	0.693	-0.063	0.128	0.685
0.05	0.696	-0.060	0.127	0.674	0.693	-0.063	0.127	0.684
0.10	0.697	-0.060	0.127	0.673	0.694	-0.062	0.127	0.682
0.15	0.697	-0.059	0.127	0.672	0.694	-0.062	0.127	0.680
0.20	0.697	-0.059	0.127	0.670	0.694	-0.062	0.127	0.680
0.25	0.697	-0.059	0.127	0.670	0.695	-0.061	0.127	0.679
0.30	0.697	-0.059	0.127	0.670	0.695	-0.061	0.127	0.678
0.35	0.697	-0.059	0.128	0.668	0.695	-0.061	0.127	0.677
0.40	0.697	-0.059	0.128	0.667	0.695	-0.061	0.127	0.676
0.45	0.698	-0.058	0.128	0.667	0.696	-0.061	0.127	0.675
0.50	0.698	-0.058	0.128	0.666	0.696	-0.060	0.128	0.674
0.55	0.698	-0.058	0.128	0.665	0.696	-0.060	0.128	0.673
0.60	0.698	-0.058	0.128	0.665	0.696	-0.060	0.128	0.671
0.65	0.698	-0.058	0.128	0.664	0.696	-0.060	0.128	0.670
0.70	0.698	-0.058	0.128	0.663	0.697	-0.060	0.128	0.669
0.75	0.698	-0.058	0.128	0.662	0.697	-0.059	0.128	0.668
0.80	0.699	-0.057	0.128	0.662	0.697	-0.059	0.128	0.667
0.85	0.699	-0.057	0.128	0.661	0.697	-0.059	0.128	0.665
0.90	0.699	-0.057	0.128	0.660	0.697	-0.059	0.128	0.664
0.95	0.699	-0.057	0.128	0.660	0.697	-0.059	0.128	0.664
1.00	0.699	-0.057	0.128	0.659	0.698	-0.058	0.128	0.663

Table 18: Albedo at S6 for initial soot concentrations of 0.002 and 0.005 ppb compared to model data for the period 2003-2015. RS2W and all statistical quantities are dimensionless.

	RSOOT = 0.002 ppb				RSOOT = 0.005 ppb			
RS2W	mean	bias	RMSE	R^2	mean	bias	RMSE	R^2
OBS	0.756	-	-	-	0.756	-	-	-
0.00	0.689	-0.067	0.129	0.692	0.682	-0.074	0.131	0.707
0.05	0.689	-0.067	0.129	0.691	0.682	-0.074	0.131	0.706
0.10	0.690	-0.066	0.128	0.689	0.683	-0.073	0.131	0.704
0.15	0.691	-0.065	0.128	0.689	0.683	-0.073	0.131	0.702
0.20	0.691	-0.065	0.128	0.688	0.684	-0.072	0.131	0.701
0.25	0.691	-0.065	0.128	0.688	0.684	-0.072	0.130	0.700
0.30	0.692	-0.064	0.128	0.687	0.685	-0.071	0.130	0.698
0.35	0.692	-0.064	0.128	0.686	0.685	-0.071	0.130	0.697
0.40	0.692	-0.064	0.128	0.685	0.685	-0.071	0.130	0.696
0.45	0.692	-0.064	0.128	0.684	0.686	-0.070	0.130	0.695
0.50	0.693	-0.063	0.128	0.682	0.686	-0.070	0.130	0.694
0.55	0.693	-0.063	0.128	0.681	0.687	-0.069	0.130	0.693
0.60	0.693	-0.063	0.128	0.680	0.687	-0.069	0.129	0.692
0.65	0.693	-0.063	0.128	0.679	0.688	-0.069	0.129	0.691
0.70	0.694	-0.062	0.128	0.678	0.688	-0.068	0.129	0.690
0.75	0.694	-0.062	0.128	0.676	0.689	-0.067	0.129	0.688
0.80	0.694	-0.062	0.128	0.674	0.689	-0.067	0.129	0.686
0.85	0.695	-0.061	0.128	0.673	0.690	-0.066	0.129	0.685
0.90	0.695	-0.061	0.128	0.671	0.690	-0.066	0.129	0.683
0.95	0.695	-0.061	0.128	0.670	0.690	-0.066	0.129	0.681
1.00	0.695	-0.061	0.128	0.669	0.691	-0.065	0.129	0.680

B.2.2 S9

Table 19: Albedo at S9 for initial soot concentrations of 0.002 and 0.005 ppb compared to model data for the period 2003-2015. RS2W and all statistical quantities are dimensionless.

	RSOOT = 0.0005 ppb				RSOOT = 0.001 ppb			
RS2W	mean	bias	RMSE	R^2	mean	bias	RMSE	R^2
OBS	0.796	-	-	-	0.796	-	-	-
0.00	0.791	-0.004	0.069	0.601	0.785	-0.010	0.070	0.602
0.05	0.796	0.001	0.071	0.579	0.788	-0.007	0.069	0.606
0.10	0.799	0.003	0.072	0.561	0.791	-0.004	0.069	0.603
0.15	0.799	0.004	0.073	0.554	0.792	-0.003	0.070	0.590
0.20	0.800	0.004	0.074	0.547	0.793	-0.003	0.071	0.579
0.25	0.801	0.005	0.074	0.548	0.794	-0.002	0.071	0.573
0.30	0.800	0.004	0.074	0.547	0.794	-0.001	0.072	0.570
0.35	0.804	0.008	0.074	0.566	0.796	-0.000	0.071	0.575
0.40	0.804	0.008	0.074	0.565	0.797	0.001	0.072	0.573
0.45	0.804	0.009	0.074	0.564	0.798	0.002	0.072	0.567
0.50	0.805	0.009	0.074	0.566	0.798	0.002	0.072	0.562
0.55	0.805	0.009	0.074	0.564	0.798	0.003	0.073	0.557
0.60	0.805	0.009	0.075	0.560	0.799	0.003	0.073	0.554
0.65	0.805	0.010	0.075	0.558	0.799	0.003	0.073	0.551
0.70	0.806	0.010	0.075	0.556	0.800	0.004	0.074	0.547
0.75	0.806	0.010	0.075	0.554	0.803	0.007	0.073	0.571
0.80	0.806	0.010	0.076	0.553	0.803	0.007	0.074	0.567
0.85	0.807	0.011	0.076	0.573	0.803	0.008	0.074	0.565
0.90	0.808	0.012	0.076	0.577	0.804	0.008	0.074	0.565
0.95	0.808	0.012	0.076	0.576	0.804	0.008	0.074	0.565
1.00	0.808	0.012	0.076	0.576	0.804	0.009	0.075	0.561

Table 20: Albedo at S9 for initial soot concentrations of 0.002 and 0.005 ppb compared to model data for the period 2003-2015. RS2W and all statistical quantities are dimensionless.

	RSOOT = 0.002 ppb				RSOOT = 0.005 ppb			
RS2W	mean	bias	RMSE	R^2	mean	bias	RMSE	R^2
OBS	0.796	-	-	-	0.796	-	-	-
0.00	0.776	-0.020	0.077	0.570	0.767	-0.029	0.079	0.590
0.05	0.780	-0.016	0.072	0.596	0.768	-0.028	0.079	0.587
0.10	0.782	-0.014	0.071	0.603	0.769	-0.027	0.078	0.583
0.15	0.783	-0.012	0.070	0.604	0.770	-0.026	0.078	0.578
0.20	0.784	-0.012	0.070	0.600	0.770	-0.025	0.078	0.575
0.25	0.785	-0.011	0.070	0.596	0.771	-0.025	0.078	0.571
0.30	0.786	-0.009	0.069	0.603	0.771	-0.024	0.078	0.569
0.35	0.787	-0.009	0.069	0.605	0.772	-0.024	0.078	0.567
0.40	0.788	-0.008	0.069	0.603	0.772	-0.024	0.078	0.564
0.45	0.789	-0.007	0.069	0.604	0.773	-0.022	0.077	0.567
0.50	0.790	-0.006	0.069	0.605	0.776	-0.020	0.074	0.589
0.55	0.791	-0.005	0.069	0.601	0.778	-0.018	0.073	0.597
0.60	0.791	-0.005	0.070	0.594	0.778	-0.018	0.073	0.595
0.65	0.792	-0.004	0.070	0.586	0.779	-0.017	0.072	0.594
0.70	0.792	-0.003	0.071	0.580	0.780	-0.016	0.071	0.604
0.75	0.793	-0.003	0.071	0.574	0.781	-0.015	0.071	0.604
0.80	0.794	-0.002	0.072	0.569	0.782	-0.014	0.071	0.603
0.85	0.796	-0.000	0.071	0.576	0.782	-0.014	0.071	0.599
0.90	0.797	0.001	0.072	0.569	0.784	-0.012	0.069	0.607
0.95	0.797	0.002	0.073	0.561	0.785	-0.011	0.069	0.605
1.00	0.798	0.002	0.073	0.556	0.786	-0.010	0.070	0.601

B.2.3 S10

Table 21: Albedo at S10 for initial soot concentrations of 0.0005 and 0.001 ppb compared to model data for the period 2009-2015. RS2W and all statistical quantities are dimensionless.

	RSOOT = 0.0005 ppb				RSOOT = 0.001 ppb			
RS2W	mean	bias	RMSE	R^2	mean	bias	RMSE	R^2
OBS	0.845	-	-	-	0.845	-	-	-
0.00	0.814	-0.032	0.061	0.455	0.810	-0.035	0.064	0.445
0.05	0.814	-0.031	0.060	0.457	0.810	-0.035	0.064	0.435
0.10	0.814	-0.031	0.060	0.457	0.811	-0.034	0.063	0.439
0.15	0.814	-0.031	0.060	0.458	0.811	-0.034	0.063	0.441
0.20	0.814	-0.031	0.060	0.460	0.812	-0.034	0.062	0.446
0.25	0.815	-0.031	0.060	0.460	0.812	-0.033	0.062	0.447
0.30	0.814	-0.031	0.060	0.460	0.812	-0.033	0.062	0.448
0.35	0.815	-0.030	0.059	0.461	0.812	-0.033	0.061	0.450
0.40	0.815	-0.030	0.059	0.462	0.813	-0.032	0.061	0.450
0.45	0.815	-0.030	0.059	0.463	0.813	-0.032	0.061	0.456
0.50	0.816	-0.029	0.058	0.467	0.813	-0.032	0.061	0.456
0.55	0.816	-0.029	0.058	0.468	0.813	-0.032	0.060	0.456
0.60	0.816	-0.029	0.058	0.465	0.814	-0.031	0.060	0.456
0.65	0.817	-0.029	0.058	0.470	0.814	-0.031	0.060	0.457
0.70	0.817	-0.028	0.057	0.474	0.814	-0.031	0.060	0.459
0.75	0.817	-0.028	0.057	0.474	0.815	-0.031	0.060	0.459
0.80	0.817	-0.028	0.058	0.470	0.815	-0.030	0.059	0.461
0.85	0.817	-0.028	0.058	0.468	0.815	-0.030	0.059	0.460
0.90	0.817	-0.028	0.058	0.465	0.815	-0.030	0.059	0.462
0.95	0.817	-0.028	0.058	0.463	0.816	-0.030	0.059	0.461
1.00	0.817	-0.028	0.058	0.459	0.816	-0.029	0.058	0.464

Table 22: Albedo at S10 for initial soot concentrations of 0.002 and 0.005 ppb compared to model data for the period 2009-2015. RS2W and all statistical quantities are dimensionless.

	RSOOT = 0.002 ppb				RSOOT = 0.005 ppb			
RS2W	mean	bias	RMSE	R^2	mean	bias	RMSE	R^2
OBS	0.845	-	-	-	0.845	-	-	-
0.00	0.805	-0.040	0.068	0.434	0.793	-0.052	0.082	0.410
0.05	0.807	-0.038	0.067	0.440	0.797	-0.048	0.075	0.440
0.10	0.807	-0.038	0.066	0.435	0.799	-0.046	0.074	0.442
0.15	0.808	-0.037	0.066	0.438	0.800	-0.045	0.072	0.450
0.20	0.808	-0.037	0.066	0.439	0.800	-0.045	0.072	0.449
0.25	0.809	-0.036	0.065	0.441	0.801	-0.044	0.071	0.450
0.30	0.809	-0.036	0.064	0.445	0.801	-0.044	0.071	0.442
0.35	0.809	-0.036	0.064	0.444	0.801	-0.044	0.071	0.444
0.40	0.810	-0.035	0.064	0.445	0.803	-0.042	0.069	0.460
0.45	0.810	-0.035	0.063	0.449	0.802	-0.043	0.070	0.444
0.50	0.810	-0.035	0.063	0.451	0.803	-0.042	0.069	0.445
0.55	0.811	-0.034	0.062	0.451	0.804	-0.041	0.068	0.446
0.60	0.811	-0.034	0.062	0.453	0.805	-0.040	0.067	0.446
0.65	0.812	-0.034	0.062	0.455	0.806	-0.039	0.067	0.445
0.70	0.812	-0.033	0.061	0.456	0.806	-0.039	0.066	0.446
0.75	0.812	-0.033	0.061	0.459	0.807	-0.038	0.065	0.448
0.80	0.813	-0.033	0.061	0.460	0.807	-0.038	0.065	0.447
0.85	0.813	-0.032	0.060	0.460	0.808	-0.037	0.065	0.445
0.90	0.813	-0.032	0.060	0.460	0.808	-0.037	0.064	0.446
0.95	0.813	-0.032	0.060	0.458	0.809	-0.036	0.064	0.448
1.00	0.814	-0.032	0.060	0.456	0.809	-0.036	0.063	0.448